Lithium Batteries

DOI: 10.1002/anie.201205569

Thermodynamics of Electrochemical Lithium Storage

*Joachim Maier**

Keywords:
defect chemistry · lithium batteries · nanotechnology · storage · thermodynamics

Dedicated to Professor John B. Goodenough on the occasion of his 90th birthday

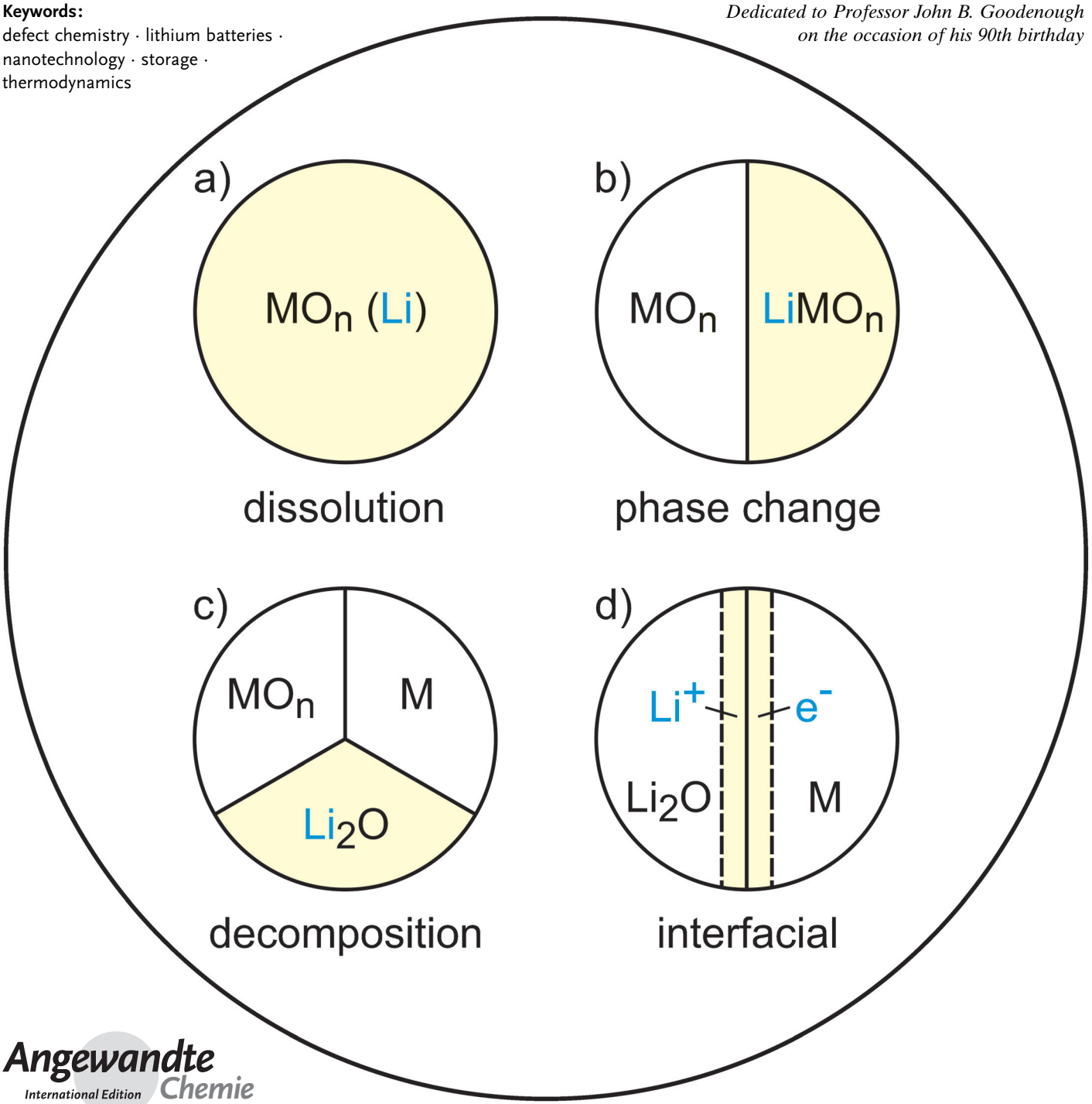

© 2013 Wiley-VCH Verlag GmbH & Co. KGaA, Weinheim

The thermodynamics of electrochemical lithium storage are examined by taking into account that it is the point defects that enable storage. While the Li defects are mobile, most of the other point defects have to be considered as frozen owing to the performance temperature being low compared to the melting point of the electrode materials. The defect chemistry needs to be considered to fully understand equilibrium charge/discharge curves. On this basis, single phase and multiphase storage mechanisms can be discussed in terms of theoretical storage capacity and theoretical voltage. Of paramount interest in the field of Li batteries are metastable materials, in particular nanocrystalline and amorphous materials. The thermodynamics of storage and voltage, also at interfaces, thus deserve a special treatment. The relationship between reversible cell voltage and lithium content is derived for the novel job-sharing mechanism. With respect to the classic storage modes, thermodynamic differences for cathodes and anodes are elaborated with a special attention being paid to the search for new materials. As this contribution concentrates on the equilibrium state, current-related phenomena (irreversible thermodynamics) are only briefly touched upon.

From the Contents

1. Introduction

Lithium-based batteries are a hot topic of current scientific debate for three reasons:

1) The need of highly reversible, high-performance batteries for a modern society. It suffices to mention two applications: a) batteries for electrotraction and b) batteries for storing electricity obtained from sustainable energy sources, mainly from sunshine or wind.[1–4]
2) The advantages arising from lithium's position in the periodic table. Lithium is characterized by its small size and high electropositivity with offer the potential of high voltage, low weight, high storage, and fast transport, and hence of high energy and power density.
3) The progress in materials science, in particular in nanotechnology, providing appropriate electrode materials characterized by highly efficient morphologies and architectures.[3,5]

This article deals with the thermodynamics of lithium storage and concentrates on the equilibrium situation (more strictly "thermostatics"). Hence the description of theoretical storage capacity and reversible cell voltage takes precedence. As questions of practical capacity and practical voltage are greatly influenced if not dominated by the specific kinetics, these will be only marginally addressed in one Section.

Why such a contribution on lithium storage, when the general thermodynamic aspects should be independent of the chemical details? First of all, there are a variety of aspects that have been specifically addressed and developed in the context of lithium-based batteries, such as storage in metastable situations and in particular in nanostructured materials.[6] They deserve special consideration. (Thus, a thermodynamic treatment of the interfacial storage mode is described for the first time in Section 6.) Moreover, even for conventional storage mechanisms, the formulation in terms of the relevant charge carriers in solids, that is, the point defects, has only been addressed in very rare cases for batteries, although this is a state-of-the-art approach in high-temperature chemistry.[7–10] This situation is quite surprising, as a full atomistic understanding as well as a pertinent physicochemical treatment is only possible on a point-defect level. In addition to the high-temperature situation, special implications of the lower temperatures, such as extensive association and relevance of frozen-in situations have to be taken account of.

In addition, the heterogeneity of the battery community makes such a contribution necessary and timely. Specialists of a certain field possibly bored by particular paragraphs might find others instructive.

There are three storage modes in solids that need to be distinguished (see Figure 1):

a) Bulk storage which is based on *dissolution* (Figure 1a). If bulk storage occurs by occupation of interstitial or vacant sites (addition) rather than by substitution it is usually

[*] Prof. J. Maier
Max Planck Institute for Solid State Research
Heisenbergstrasse 1, 70569 Stuttgart (Germany)
E-mail: s.weiglein@fkf.mpg.de

© 2013 Wiley-VCH Verlag GmbH & Co. KGaA, Weinheim

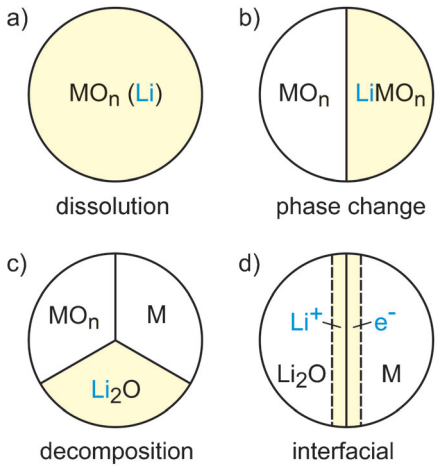

Figure 1. The storage mechanisms, as discussed in the text.

called insertion (or if these interstitial sites are between defined layers, intercalation). In this storage mode the phase stays constant (single phase storage), so only a variation in the point-defect chemistry occurs (storage in TiS_2 or $LiCoO_2$ are examples).[11,12]

b) Storage that accompanies *phase changes*. In this case the chemistry of the perfect structure is altered, while the defect chemistry is invariant. Since the co-existing phases exhibit and maintain their extreme non-stoichiometries, the defect chemistry is still relevant. As far as kinetics is concerned, it is pertinent to distinguish between phase transformation reactions (e.g. $FePO_4/LiFePO_4$)[13] and decomposition reactions (e.g. $LiCoO_2$ decomposing to Co and Li_2O on excessive lithiation)[14–19] depending on the complexity of the composition trajectory in the phase diagram (see Figure 1 b,c). The decomposition is also referred to as a (proper) conversion reaction.

c) Lithium can also be stored at higher-dimensional defects, in particular at *interfaces*. This storage can be due to the special structure of the interfacial core, but is possible even in the case of an ideal abrupt two-phase contact ("job-sharing" mechanism)[20–22] shown in Figure 1 d. Examples are nanocomposites of metals (e.g. Ru) and lithium oxide. This job-sharing mechanism as well as the conversion reaction mechanism relies on nanostructuring. (But also in the classic cases of single-phase or two-phase storage nanoparticles are beneficial whenever bulk-transport within the solid is sluggish.) In a certain sense, even though referring to bulk, Li storage in frozen-in one-dimensional or even zero-dimensional defects may be mentioned as well, examples being Li storage in dislocation cores of plastic materials or in C-vacancies of carbon-based materials.[23]

Joachim Maier studied chemistry at the University of Saarbrücken (Ph.D. 1982), and completed his habilitation at the University of Tübingen (1988). He is or has been a lecturer at Tübingen, a foreign faculty member at MIT, a visiting professor at the University of Graz, and an honorary professor at the University of Stuttgart. As director of the department of physical chemistry of solids (since 1991) of the Max Planck Institute for Solid State Research his concern is the understanding of chemical and electrochemical phenomena involving solids and their use in materials science.

2. Electrical Exploitation of the Chemical Potential in a Battery

The comparison of a battery with a pumped-storage hydropower plant is instructive. In a pumped-storage hydropower plant, whenever energy needs to be stored, water is pumped from the lower level to the higher level. The energy can be released by allowing the water to flow from the higher level to the lower level and to do work (see Figure 2 a).

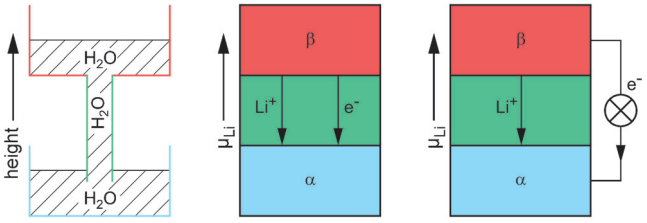

Figure 2. The principle of a hydropower plant (left) as compared with a principle of a lithium battery (right). Center: If the green phase was a mixed conductor rather than an electrolyte, an irreversible reaction would take place and only heat would be generated.

In a (lithium) battery we are not concerned with the gravitational potential[24] but with the chemical potential (of lithium, μ_{Li}). The chemically stored energy is exploited which per given mass is exceedingly greater than in the previous example.[25] During charge we "pump" the neutral component—lithium—from a phase α (the positive electrode)[26] to a phase β where Li is less welcome (the negative electrode).[26] In other words, we pump Li from a level of lower chemical potential to a level of higher chemical potential. Note that the chemical potential is according to its definition ($\mu_{Li} = \partial G/\partial n_{Li}$, with pressure, temperature, and mole numbers of other components staying constant, G: Gibbs energy) a measure of how much a component is "disliked" in a given phase.

Exploiting chemical potential differences, and not gravitational potential differences and hence dealing with exceedingly greater energy densities, is not the only conceptual difference. A neutral Li transport from the high potential side to the low potential side would only produce heat (corresponding to the usually very negative reaction enthalpy $\Delta_R H$), the conversion of which into electrical energy would be limited by Carnot's efficiency. A battery device uses the trick to split the Li flow into an internal Li^+ ion flow and an outer e^- flow, which is enabled by placing a Li^+ ion conducting electrolyte between the two reservoirs (electrodes) as displayed in Figure 2. The electrons in the outer circuit can perform electrical work directly. This arrangement allows for a very elegant and reversible transformation of chemical

© 2013 Wiley-VCH Verlag GmbH & Co. KGaA, Weinheim

energy into electrical energy and vice versa. Moreover, since now the total driving force in form of the free enthalpy of the reaction (R), $\Delta_R G$, is transformed into electrical energy, the theoretical efficiency is given by $\Delta_R G/\Delta_R H = 1 + T\Delta_R S/|\Delta_R H|$ and is in principle allowed to exceed 100% (if $\Delta_R S > 0$; the surrounding environment cools down); usually it is around 100% as the reaction entropy $\Delta_R S$ is small.

If the outer circuit is interrupted, a reversible cell voltage (E) builds up that equals $-\Delta_R G/z_R F$ (F: Faraday's constant). (Here it is, as usual, silently understood that the reaction quantities, in contrast to G above, refer to molar units.) This assumes absence of any internal dissipative processes, such as local corrosion or electrochemical short-circuit enabled by non-negligible electronic transport in the electrolyte. The number of transferred electrons in the reaction R, that is, z_R, equals unity if we write the reaction in the general form:

$$\mathrm{Li}(\beta) \rightarrow \mathrm{Li}(\alpha) \tag{1}$$

This overall reaction is not in global chemical equilibrium, but under the reversible conditions of an open electrochemical cell in a constrained equilibrium state ("electrochemical equilibrium"). Basic electrostatics tells us that the voltage (multiplied by Faraday's constant) equals the difference in the Fermi potentials (electrochemical potentials of electrons, $\tilde{\mu}_{e^-}$) of the terminal copper leads.[27]

At the electrodes local chemical equilibrium between Li and Li^+, e^-

$$\mathrm{Li} \rightleftharpoons \mathrm{Li}^+ + \mathrm{e}^- \tag{2}$$

demands

$$\tilde{\mu}_{\mathrm{Li}^+} + \tilde{\mu}_{\mathrm{e}^-} = \mu_{\mathrm{Li}} \tag{3}$$

As in the case of the electrons, $\tilde{\mu}$, denotes the electrochemical potential, that is, the chemical potential complemented by the electrical potential term $zF\Delta\phi$ (for a neutral component such as Li $z=0$ and hence $\tilde{\mu}=\mu$). As the electrolyte conducts Li^+ and not e^-, there are no gradients in $\tilde{\mu}_{\mathrm{Li}^+}$.[28] If we compare the situation at the two electrodes, then $\Delta\tilde{\mu}_{e^-} = \Delta\mu_{\mathrm{Li}}$ and hence

$$-EF = \tilde{\mu}_{\mathrm{e}^-}(\alpha) - \tilde{\mu}_{\mathrm{e}^-}(\beta) = \mu_{\mathrm{Li}}(\alpha) - \mu_{\mathrm{Li}}(\beta) \tag{4}$$

stating again that it is the difference in the chemical potential of Li that is exploited. If one wants to avoid confusion between electrochemical and chemical equilibrium, one can write the cell reaction Equation (1) as

$$\mathrm{Li}(\beta) + \mathrm{e}^-(\alpha) \rightleftharpoons \mathrm{Li}(\alpha) + \mathrm{e}^-(\beta) \tag{5}$$

to which the equilibrium conditions (zero balance of electrochemical potentials) can now safely be applied.[10,29] Equation (5) expresses the fact that an electrochemical equilibrium cell is characterized by local electrode equilibrium, but globally it is only the ions but not the electrons that are in equilibrium under open-circuit conditions.

In the following it is useful to refer to reversible voltages E with respect to metallic Lithium as negative electrode, that is, we define the phase β as solid lithium (Li(s)) giving Equation (6).

$$\begin{aligned} EF &= -\left(\mu_{\mathrm{Li}}(\alpha) - \mu^\circ_{\mathrm{Li}}(\mathrm{Li})\right) \\ &= -\mu^\circ_{\mathrm{Li}}(\alpha) - RT\ln a_{\mathrm{Li}}(\alpha) + \mu^\circ_{\mathrm{Li}}(\mathrm{Li}) \\ &= -RT\ln a_{\mathrm{Li}}(\alpha) - \left(\mu^\circ_{\mathrm{Li}}(\alpha) - \mu^{\circ\circ}_{\mathrm{Li}}\right). \end{aligned} \tag{6}$$

As usual we have split μ into a standard value μ° and a concentration (c) dependent term in which $a(c)$ denotes the activity; the standard potential in our reference electrode Li(s) is abbreviated as $\mu^{\circ\circ}_{\mathrm{Li}} \equiv \mu^\circ_{\mathrm{Li}}(\mathrm{Li})$ $(= \mu_{\mathrm{Li}}(\mathrm{Li}))$. According to Equation (6) E is determined by $\ln a$ but also includes the free energy of virtually transferring one mole Li from the metal to the phase α at $a=1$.

All the different storage modes addressed above can be observed in a material such as RuO_2.[16,30,31] Let us first assume that the RuO_2 entity (X) behaves as an invariant component under experimental conditions, that is, we ignore variations of the Ru/O ratio. This idealization—which is a typical room-temperature assumption—enables $Li_\xi RuO_2$ to be conceived as a pseudo-binary ($Li_\xi X$). The experimental discharge/charge curve in Figure 3 is not exactly the current-less

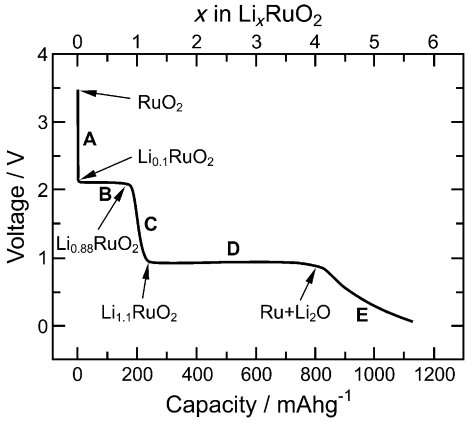

Figure 3. The discharge profile of RuO_2, exhibiting all the relevant storage modes: single-phase storage (A,C), two-phase storage (B), decomposition (D) as well as interfacial storage (E). Reproduced from Ref. [17].

situation but close to it. This curve is obtained by adding Li to the system keeping the amount of X constant. Irrespective of the complexity of the processes possible, on Li addition the electromotive force (e.m.f.) will decrease towards zero and the Li potential increase towards $\mu^{\circ\circ}_{\mathrm{Li}}$. This follows from the thermodynamic stability criterion $\partial\mu_{\mathrm{Li}}/\partial n_{\mathrm{Li}} > 0$.[32]

Starting out from RuO_2, the phase first dissolves Li up to about $\xi = 0.1$. During this process the chemical potential of Li increases continually until the $LiRuO_2$ phase is formed. During the single-phase process it is δ, the deviation of ξ from the composition of order (cf. $Li_{1+\delta}RuO_2$), that is, from the "Dalton-composition" (cf. Li_1RuO_2), as well as μ_{Li}, the lithium potential (and then also a_{Li}, the Li activity), which are decisive for capacity and voltage, respectively. It is

© 2013 Wiley-VCH Verlag GmbH & Co. KGaA, Weinheim

emphasized below how these functions are, for a given phase, interlinked through point-defect chemistry.

If the Li solubility is exceeded, the phases $Li_{0.1}RuO_2$ and $Li_{0.9}RuO_2$ coexist. During this process, it is not the compositions in the phases but only the fractions of these phases that will vary until all the RuO_2 is converted into $LiRuO_2$. In this period μ_{Li} and hence the voltage stays invariant. Unlike the coexistence compositions of the phases, the overall composition "$Li_\xi RuO_2$" does vary. Naturally this overall value of ξ defines the capacity.

After this point additional Li is taken up by the $LiRuO_2$ phase (up to $Li_{1.1}RuO_2$) until a new phase equilibrium is established. Unlike the transformation from RuO_2 to $LiRuO_2$ which follows a straight line in the Li-Ru-O phase diagram, the trajectory bifurcates and $LiRuO_2$ decomposes into Ru and Li_2O. Thus we have to realize that we are dealing with a ternary mixture. (The low mobilities of Ru and O express themselves in the nano- and sub-nanostructure of the Ru/Li_2O composite formed on decomposition.) In the invariant regime $Li_{1.1}RuO_2$, Ru, and Li_2O coexist. (Reversal of this process is kinetically much more demanding but may be possible if the particles are very tiny and the transport coefficients not too small.[16] Such a reversal has indeed been verified for RuO_2.)[17] The only bulk process before plating of Li occurs, is an alloy formation (a further single-phase process), which in the case of Ru is negligible.

Owing to the large interfacial proportion realized in the above phase mixture, a very interesting storage mode emerges in which Li is stored heterogeneously at the Ru/Li_2O contacts, namely by accommodating Li^+ on the Li_2O side and e^- on the Ru side of the contact.[17,20–22] Owing to heterogeneity, the thermodynamic behavior is quite different from the normal storage mode. Again the Li potential determines E, and the overall composition determines the capacity, but unlike μ_{Li} the Li content is a composite function in this heterogeneous problem.[22] If all the possibilities to stabilize Li (compared with the pure Li metal) are exhausted, Li plating occurs. Note that for very thin layers μ_{Li} may be slightly smaller than the lithium potential of pure lithium $\left(\mu_{Li}^{\circ\circ}\right)$ which serves a counter electrode. This underpotential deposition can of course also be viewed as interfacial storage. Let us address the major storage modes—in our open-circuit cell with elemental Li as negative electrode—step by step.

3. Solid Solution Storage and Defect Chemistry

Unlike Equation (1) [but like Eq. (2)] we now consider the local equilibrium situation in the working electrode. Incorporation of Li in the bulk of the phase α can be written as

$$Li \rightleftharpoons Li(\alpha) \tag{7}$$

which in chemical equilibrium requires

$$\mu_{Li} = \mu_{Li}(\alpha) \tag{8}$$

or in terms of activities (mass-action law level; $\mu_{Li} \equiv \text{const} + RT\ln a_{Li}$)

$$a_{Li} \propto a_{Li}(\alpha) \tag{9}$$

In Equations (8,9), μ_{Li} is the chemical potential (and a_{Li} the activity) of the working electrode side and may be identified with the Li potential in the virtual local equilibrium gas-atmosphere (differing from the Li potential at the counter electrode by EF).[33]

Knowing that in an ionic material Li is at least partly dissociated into Li^+ and e^-, that is

$$Li \rightleftharpoons Li^+(\alpha) + e^-(\alpha) \tag{10}$$

we write

$$\mu_{Li} = \mu_{Li}(\alpha) = \mu_{Li^+}(\alpha) + \mu_{e^-}(\alpha) \tag{11}$$

or

$$a_{Li} \propto a_{Li}(\alpha) = a_{Li^+}(\alpha) \cdot a_{e^-}(\alpha) \tag{12}$$

whereby $\mu_{Li} - \mu_{Li}^{\circ\circ}$ determines the e.m.f.

Much more detailed information can be arrived at on the level of the point defects. There are two mechanistic ways of incorporating Li into the solid.[33–36] The first is bringing Li^+ into an interstitial site of the lattice according to Equation (13).

$$Li + \text{empty interstitial site} \rightleftharpoons \text{interstitial } Li^+ + \text{excess } e^- \tag{13}$$

In Kröger–Vink nomenclature which uses relative charges (dot, cross, and prime stand for the relative charges $+1$, 0 and -1), this reads (V: vacancy, i: interstitial site) as:

$$Li + V_i^x \rightleftharpoons Li_i^\bullet + e' \tag{14}$$

Alternatively, Li^+ may occupy a vacancy according to:

$$Li + Li^+\text{-vacancy} \rightleftharpoons \text{regular } Li^+ + \text{excess-}e^- \tag{15}$$

or in Kröger–Vink notation:

$$Li + V'_{Li} \rightleftharpoons Li_{Li}^x + e' \tag{16}$$

One of the two equations will be redundant if we take into consideration the ionic (Frenkel) disorder equilibrium:

$$\text{regular } Li^+ + \text{empty interstitial site} \rightleftharpoons Li^+ + Li^+\text{-vacancy} \tag{17}$$

that is

$$Li_{Li}^x + V_i^x \rightleftharpoons Li_i^\bullet + V'_{Li}. \tag{18}$$

Similarly, we do not need to reformulate all the Equations with electron holes instead of excess electrons (conduction electrons). It suffices to add to our list the electronic disorder equilibrium Equation (19)

 © 2013 Wiley-VCH Verlag GmbH & Co. KGaA, Weinheim

$$\text{electron (valence band)} + \text{hole (conduction band)} \rightleftharpoons \text{electron (conduction band)} + \text{hole (valence band)} \tag{19}$$

or in Kröger–Vink nomenclature:

$$\text{Nil} \rightleftharpoons e' + h^{\bullet} \tag{20}$$

The great thermodynamic advantage of formulating the situation in the model compound "LiX" (which more precisely reads $Li_{\xi}X \equiv Li_{1+\delta}X$ with $\delta \ll 1$) in terms of point defects, is that now ideal mass-action laws are good approximations because defects (unlike components) are rather dilute ($a \simeq c$).

Non-idealities (that we largely ignore) can be corrected for by introducing activity coefficients.[37–39] Furthermore the distinction between excess and deficient particles allows a detailed calculation of $\delta(E)$, that is, of the theoretical charge/discharge curve. Neglecting activity coefficients the following set of mass-action Equations is sufficient up to this point[40]

$$K_{Li} = [Li_i^{\bullet}][e']a_{Li}^{-1} \tag{21}$$

$$K_F = [Li_i^{\bullet}][V'_{Li}] \tag{22}$$

$$K_B = [e'][h^{\bullet}]. \tag{23}$$

These mass action laws follow from Equations (14), (18), (20) by applying the balance of the chemical potentials

$$\mu_{Li} = \mu_i + \mu_n = -\mu_V + \mu_n = -\mu_V - \mu_p \tag{24}$$

If coupled with the electroneutrality condition the defect concentrations and also δ can be calculated as a function of Li activity and hence of cell voltage.

The electroneutrality condition is given as

$$C + [Li_i^{\bullet}] + [h^{\bullet}] = [V'_{Li}] + [e'] \tag{25}$$

where C stands for the effective concentration of charged impurities (dopants). C is positive if we refer to higher-valent cations such as Mg^{2+} on Li^+ site, that is, $Mg_{Li}^{\bullet}$. C is negative if we refer to higher-valent anions, for example, Z^{2-} on an X^- site, that is, Z'_X; an example being O^{2-} replacing F^-. In addition, C also includes the concentration of charged frozen native point defects. Examples for such defects are iron vacancies in $LiFePO_4$, anti-site defects, such as $Fe_{Li}^{\bullet}$ therein, or oxygen vacancies in TiO_2 which are considered to be immobile at room temperature. The appearance of frozen-in native defects is one characteristic feature of room-temperature defect chemistry. The reader interested in the interconnection of frozen concentrations in the temperature range of performance and variable concentrations in the temperature range of preparation is referred to the literature.[41,42] A second characteristic feature of room-temperature defect chemistry is the increased tendency to association of oppositely charged defects,[33] such as native interactions

$$V'_{Li} + h^{\bullet} \rightleftharpoons V_{Li}^{x}$$
$$Li_i^{\bullet} + e' \rightleftharpoons Li_i^{x} \tag{26}$$

or association reaction with impurities

$$Mg_{Li}^{\bullet} + V'_{Li} \rightleftharpoons (Mg_{Li}V_{Li})^{x}$$
$$Z'_X + Li_i^{\bullet} \rightleftharpoons (Li_iZ_X)^{x} \tag{27}$$
$$Z'_X + h^{\bullet} \rightleftharpoons Z_X^{x}$$

(Elastic interaction may even lead to association between equally charged defects. Cooper pairs are the most prominent examples of "anti-Coulombic" association.)

Taking account of association reactions means adding further mass-action laws to our list [Eq. (21)]. Neutral associates do not appear in the electroneutrality equation. In such cases, C in Equation (25) is no longer constant and explicit consideration of the mass balances is required. Such solutions are state of the art in defect chemistry and the interested reader finds a great number of examples in Refs. [7,8,10,43,44].

Figures 4, 5, 7 and 8 show how the defect concentrations depend on the lithium activity if, for simplicity, association reactions have been neglected. These solutions are based on the so-called Brouwer conditions[45] which means that in the various segments only two majority carriers of opposite charge are of relevance in Equation (25). This approach leads to power laws for the concentrations or linear graphs in the log-log plots. Note that significant variations in the log-log plots refer to order of magnitude variations.

Five cases are considered: 1) a pure material (termed LiX) with intrinsically predominant ionic disorder, 2) a pure material (termed LiY) with intrinsically predominant electronic disorder; 3,4) LiX and LiY being donor doped, and 5) finally the acceptor-doped case for the example of predominant ionic disorder (LiX).

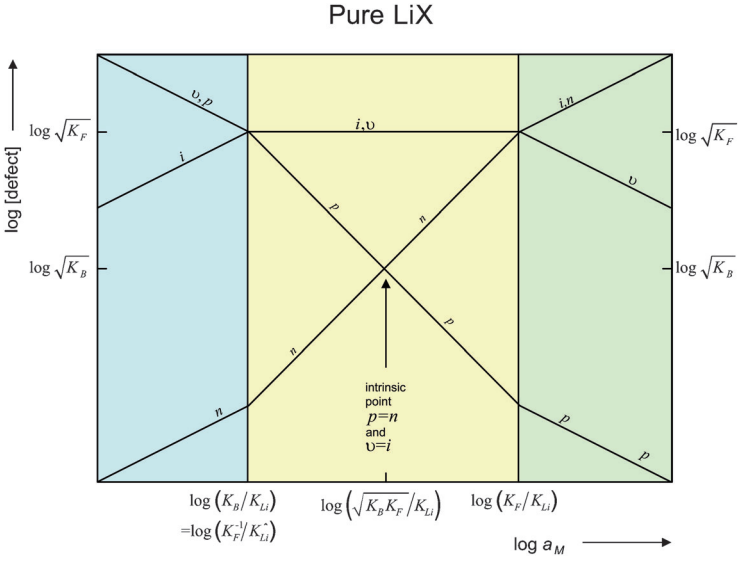

Figure 4. Defect chemistry and defect chemical parameters for an intrinsically mainly ionically disordered (pseudo-) binary Li compound. I regime (yellow), P regime (blue), N regime (green).

© 2013 Wiley-VCH Verlag GmbH & Co. KGaA, Weinheim

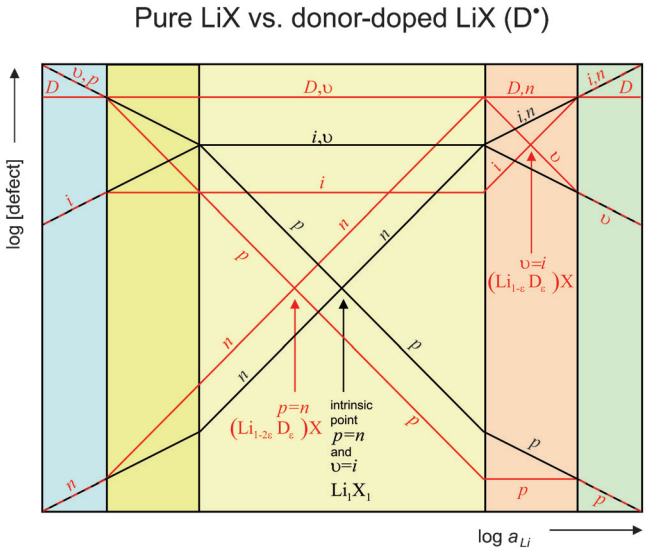

Figure 5. Defect chemistry of a pure (black curves) and donor doped (red curves) (pseudo-)binary Li compound with intrinsically predominant ionic disorder. I regime (light yellow), P regime (blue), N regime (green), C_I regime (yellow), C_E regime (red).

Notwithstanding the fact that the individual defect concentrations are highly relevant for the kinetic aspects of ionic and electronic transport, we are interested in the thermostatics of Li storage and thus in the equilibrium lithium content $1+\delta$ as a function of voltage and hence of lithium activity a (where for simplicity the index Li has been dropped). If we can ignore point defects in the X sublattice, the "non-stoichiometry" δ is given by the concentration of interstitial lithium species minus the concentration of lithium vacancies.

Let us consider first the pure material: In this case electroneutrality demands $\delta = i - v = n - p$. (From here on we use the abbreviations i, v, n, p for $[Li_i^\bullet]$, $[V'_i]$, $[e']$, $[h^\bullet]$, respectively.) For Brouwer conditions, power laws result in terms of the lithium activity as typical mass-action-law solutions; that is, for any defect j it holds that $[j] \propto a^{N_j}$ (where N_j is a simple rational number).[45] If ionic disorder is predominant, the logarithmic dependence, that is, the relative variation, of the already significantly disordered majority carrier concentrations on a is small, hence $N_i = N_v = 0$ [follows from Eqs. (22), (25), cf. Figure 4] but $N_n = 1 = -N_p$ [follows from Eqs. (22), (23), cf. Figure 4]. Writing $\delta = i - v$ simply delivers $\delta \simeq 0$ on this level of approximation. A better approximation is obtained by replacing $i - v$ by $n - p$ and analyzing the minority defects. The fact that δ can be written as a difference of two terms with inverse dependencies on a, that is, $\delta = \alpha a^N - \beta a^{-N}$ leads to a sinh-function in terms of the e.m.f [cf. Eq. (6)].[46] In such cases δ can favorably be recast in the form $c^*\left((a/a^*)^N - (a/a^*)^{-N}\right)$ with $c^* = \sqrt{\alpha\beta}$ and $a^* = (\beta/\alpha)^{\frac{1}{2N}}$. In the present case c^* turns out to be the n- or p-concentration at the stoichiometric point [see Figure 4, middle; Eq. (28)]

$$c^* \equiv n^* \equiv n(\delta = 0) = p^* \equiv p(\delta = 0) \tag{28}$$

At this point the composition $Li_{1+\delta}X$ is realized with δ strictly equal to 0. The corresponding activity is termed a^*.

To translate these graphs into the battery relevant representation of e.m.f. versus Li content which reflects the equilibrium charge/discharge curve, it is useful to simplify notation by abbreviating EF/RT by $\mathcal{E}$ and to refer to the stoichiometric point, that is, $\mathcal{E} - \mathcal{E}^* = -\ln(a/a^*)$ with $\mu_{Li} \equiv \text{const} + RT \ln a_{Li}$ and $\mathcal{E}(a^*) \equiv \mathcal{E}^*$.

For the special case of predominant ionic disorder (I range) the defect chemical situation gives:

$$\delta = c^*\left(\left(\frac{a}{a^*}\right) - \left(\frac{a}{a^*}\right)^{-1}\right) \tag{29}$$

with $c^* = \sqrt{K_B}$ and $a^* = K_B^{1/2} K_F^{1/2} \Big/ K_{Li}$.

The pure, predominantly electronic case realized in LiY (black curves in Figure 8, E regime) yields structurally the same result as for the predominantly ionic case realized in LiX, but $c^* = \sqrt{K_F}$. Using $\mathcal{E}$ we can formulate in both cases [Eq. (30)]

$$\delta = 2c^* \sinh -(\mathcal{E} - \mathcal{E}^*) \tag{30}$$

representing the well-established s-shaped titration curve as for example, realized for $LiRuO_2$ in Figure 3 (cf. zone labeled C).

So far we have concentrated on the regime near the stoichiometric point (I regime; yellow in Figure 4). For very low or high Li activities the material is significantly oxidized (P regime, blue in Figure 4) or reduced (N regime, green in Figure 4) with respect to the intrinsic composition. Then the carriers generated by Li excess or deficiency dominate.

Thus, in the N regime ($a \gg a^*$) it is $Li_i^\bullet$ and e' and in the P regime ($a \ll a^*$) V'_{Li} and $h^\bullet$ that form the majority carriers. In each regime we can neglect v or i in the difference $i - v$ with the result

$$\begin{aligned} \delta &\simeq K_{Li}^{1/2} a^{1/2} = K_F^{1/4} K_B^{1/4} (a/a^*)^{1/2} \propto \exp\left[-\frac{\mathcal{E} - \mathcal{E}^*}{2}\right] \qquad (\text{for } a \gg a^*) \\ \delta &\simeq -K_B^{1/2} K_F^{1/2} K_{Li}^{-1/2} a^{-1/2} \\ &= -K_F^{1/4} K_B^{1/4} (a/a^*)^{-1/2} \propto -\exp\left[-\frac{\mathcal{E} - \mathcal{E}^*}{2}\right] \qquad (\text{for } a \ll a^*) \end{aligned} \tag{31}$$

These equations hold for both LiX and LiY.

It is at this point worthy of mention that the defect chemical knowledge also allows the free energy to be formulated as a function of the stoichiometry. This is outlined in Appendix I b.

Returning to the defect concentrations. If we aim at a more general treatment, we have to give up the Brouwer approximation, that is, to apply the full electroneutrality equation Equation (25) (as we still refer to pure material $C = 0$).

The results for the individual carrier concentrations are

$$i = \sqrt{\frac{(aK_{Li} + K_F) aK_{Li}}{(aK_{Li} + K_B)}} = K_F/v = aK_{Li}/n = (aK_{Li}/K_B)p \tag{32}$$

© 2013 Wiley-VCH Verlag GmbH & Co. KGaA, Weinheim

and then for the overall composition

$$\delta = \sqrt{\frac{(aK_{Li}+K_F)aK_{Li}}{aK_{Li}+K_B}} - K_F\sqrt{\frac{aK_{Li}+K_B}{(aK_{Li}+K_F)aK_{Li}}} \tag{33}$$

Equation (33) will be exploited in Section 8 in more detail.

For $aK_{Li} \gg K_F, K_B$ the above results [Eq. (31)] for the N regime are reproduced as they are for $aK_{Li} \ll K_F, K_B$ for the P regime. The sinh solution for the I regime is reproduced if $K_F \gg aK_{Li} \gg K_B$ (ionic disorder) or $K_F \ll aK_{Li} \ll K_B$ (electronic disorder). Also the transition values for a and δ are easily found. In the case of a material with predominant ionic disorder, one obtains $a_{I/N} = K_F/K_{Li}$ and $\delta_{I/N} = \sqrt{K_F/2}$ for the transition from I to N while for the transition from I to P, $a_{P/I} = K_B/K_{Li}$ and $\delta_{P/I} = -\sqrt{K_F/2}$ result.

Figure 6 displays the respective $\mathcal{E}$ versus δ curve for the intrinsically ionically disordered LiX for the total activity range (P, I, and N regime). It also shows the limits δ_{max}, δ_{min} given by phase competition (cf. Section 8). Also shown (dashed lines) are variations due to defect saturation addressed at the end of the Section.

A characteristic feature of the pure material (cf. Figure 4) is that at the point where the ionic defect concentrations precisely coincide, the electronic concentrations are equal as well.

According to Equation (25) these points differ if the material is doped. On the concentration scale this difference is C. So let us turn to the doped situation and investigate magnesium-doped LiX or LiY as examples.

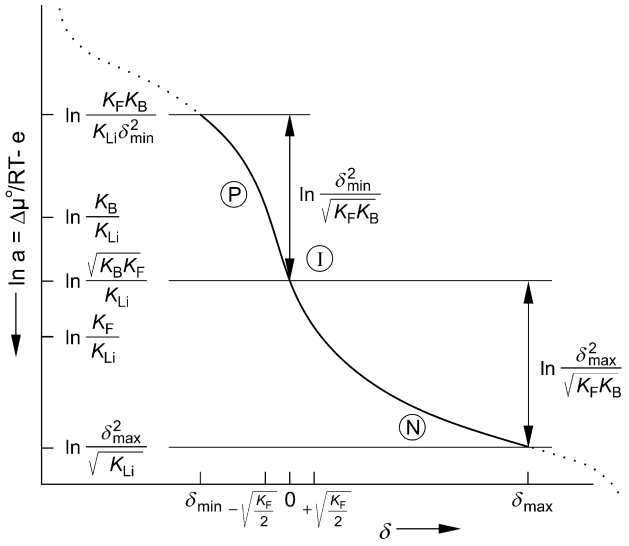

Figure 6. The lithium activity (cell voltage) versus Li content δ for a dissolution mechanism, for a mainly ionically disordered crystal. The defect-chemical partners are calculated from Equation (33). Before site exhaustion becomes relevant, which would severely limit further extraction or incorporation of Li (see dashed part), the phase transforms into coexisting phases (δ_{min}, δ_{max}). Note that usually the dashed range is much more extended than shown here. $\Delta\mu^\circ$ = partial molar free enthalpy change during the transfer of a Li from the electrode phase to metallic lithium under standard conditions.

Figure 5 shows, for the LiX example, how the activity (a^*_{eon}), where $p = n$, differs from the activity (a^*_{ion}), where $v = i$. Let $Li_\xi Mg_\varepsilon X$ be the composition with variable ξ, then the composition at $a = a^*_{eon}$ where the dopant is completely compensated by the ionic defects, is $Li_{1-2\varepsilon}Mg_\varepsilon X$ ($[Mg^\bullet_{Li}] \simeq [V'_{Li}]$). At $a = a^*_{ion}$ the composition is $Li_{1-\varepsilon}Mg_\varepsilon X$ and the dopant is purely electronically compensated ($[Mg^\bullet_{Li}] \simeq [e']$), formally by a lower Li valence and/or more negative X valence.

The inequality $a^*_{eon} < a^*_{ion}$ holds generally for donor doping no matter if the donor effect is caused by higher-valent substitutional cations, lower-valent substitutional anions, by interstitial cations, or positively charged frozen-in native defects. It also holds if the disorder is primarily electronic (see Figure 8).

Exactly the opposite occurs for acceptor doping (see Figure 7). In the example that X^- is partially substituted by Z^{2-} ($Li_\xi X_{1-\varepsilon}Z_\varepsilon$) the composition at a^*_{eon} is $Li_{1+\varepsilon}X_{1-\varepsilon}Z_\varepsilon$ (ionic compensation) and $Li_1X_{1-\varepsilon}Z_\varepsilon$ at a^*_{ion} (electronic compensation). (The inequality $a^*_{eon} > a^*_{ion}$ also holds true for lower valence substitutional cations, for interstitial anions, or effectively negatively charged frozen-in native defects.) The asymmetry introduced by the dopant is not only reflected by the non-zero gap between a^*_{eon} and a^*_{ion}, but also by the pronounced asymmetry of the defect concentrations as functions of a (cf. Figure 5, 7, and 8).

If now, unlike Equation (32), we take account of the effective doping content C in the electroneutrality equation, we arrive at Equation (34)

$$i = -\frac{C}{2\left(1+\frac{K_B}{K_{Li}}\frac{1}{a}\right)} + \sqrt{\frac{C^2}{4\left(1+\frac{K_B}{K_{Li}}\frac{1}{a}\right)^2} + \frac{K_{Li}a + K_F}{\left(1+\frac{K_B}{K_{Li}}\frac{1}{a}\right)}} \tag{34}$$
$$= K_F/v = K_{Li}\,a/n = p(aK_{Li}/K_B)$$

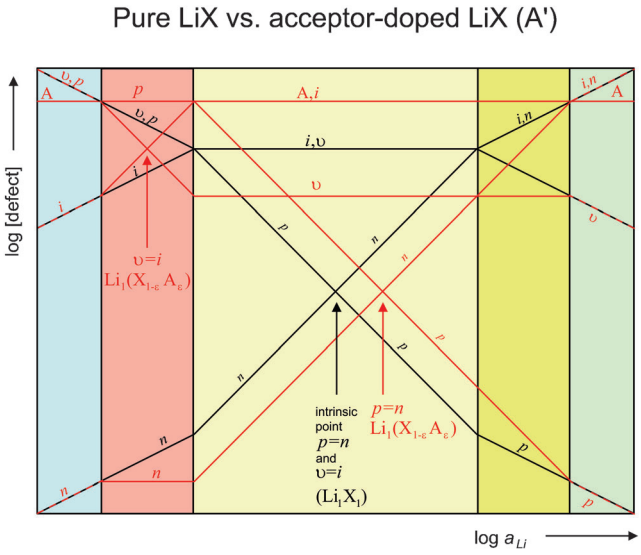

Figure 7. Defect chemistry of a pure (black curves) and acceptor doped (red curves) (pseudo-) binary Li compound with intrinsically predominant ionic disorder. I regime (light yellow), N regime (blue), P regime (green), C_I regime (yellow), C_E regime (red).

© 2013 Wiley-VCH Verlag GmbH & Co. KGaA, Weinheim

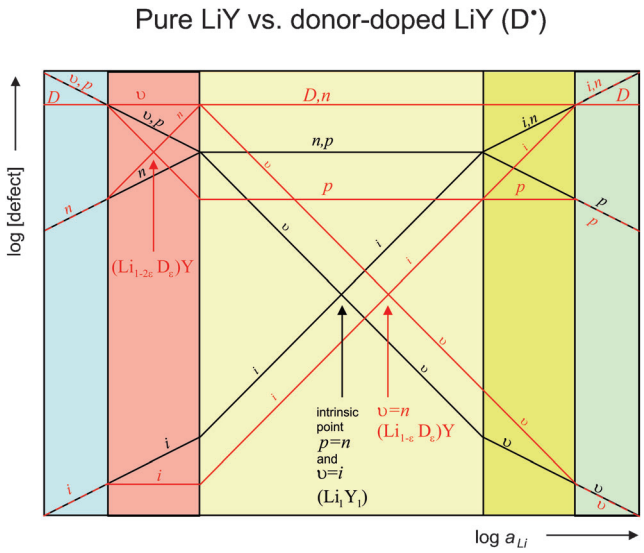

Figure 8. Defect chemistry of a pure (black curves) and donor doped (red curves) (pseudo-) binary Li compound with intrinsically predominant electronic disorder. E regime (light yellow), N regime (blue), P regime (green), C_E regime (yellow), C_I regime (red).

as solutions for the individual defect concentrations. From these individual concentrations the non-stoichiometry is directly obtained.

Numerical solutions of Equation (34) will be exploited in Section 8.

As far as the parameter a^*_{eon} is concerned (here $n=p$, hence $C+i=v$), it follows that

$$a^*_{eon}=\frac{\sqrt{K_B}}{K_{Li}}\left(-\frac{C}{2}+\sqrt{\frac{C^2}{4}+K_F}\right) \tag{35}$$

while for a^*_{ion} (here $i=v$, hence $C+p=n$)

$$a^*_{ion}=\frac{\sqrt{K_F}}{K_{Li}}\left(\frac{C}{2}+\sqrt{\frac{C^2}{4}+K_B}\right) \tag{36}$$

and thus for the difference

$$a^*_{ion}-a^*_{eon}=\frac{C}{K_{Li}}\left[\sqrt{K_F}\left(\frac{1}{2}+\mathrm{sgn}C\sqrt{\frac{1}{4}+\frac{K_B}{C^2}}\right)-\sqrt{K_B}\left(-\frac{1}{2}+\mathrm{sgn}C\sqrt{\frac{1}{4}+\frac{K_F}{C^2}}\right)\right] \tag{37}$$

The bracked term is positive ($\sqrt{K_F}$ for $C\to\infty$, $\sqrt{K_B}$ for $C\to-\infty$), hence

$$\frac{a^*_{ion}-a^*_{eon}}{C}>0 \tag{38}$$

proving that $a^*_{ion}>a^*_{eon}$ for donor doping ($C>0$) and $a^*_{ion}<a^*_{eon}$ for acceptor doping ($C<0$). In the definition of δ we have the freedom to either consider the deviation from the composition at a^*_{ion} or from the composition at a^*_{eon}, that is, to refer to $\delta_{ion}\equiv i-v$ or to $\delta_{eon}\equiv n-p$. (This question of reference state is of course not of relevance for the amount of Li storage.) In both cases the activity dependence follows from Equation (34).

As already mentioned, now, unlike the undoped situation, δ_{eon} is different from δ_{ion} by

$$\delta_{eon}-\delta_{ion}=C>0 \tag{39}$$

Let us consider the special Brouwer regimes and hence special cases of Equation (34). The N and P regimes trivially lead to the same results as for the pure material since there C is negligible with respect to the native concentrations. But the situation is different for the regime in between, which, in the pure case, was termed the I regime for LiX and the E regime for LiY, and in which the dopant is now a majority carrier. In the doped case both types of regimes can occur in the same material (see Figures 5, 7, 8), that is, a regime in which all the electronic carriers are minority carriers (termed C_I regime) as well as a regime wherein all ionic carriers are in minority (termed C_E regime). It is instructive to consider the ionically compensated regime (C_I) and the electronically compensated regime (C_E) separately.

In the first case it holds that $C\simeq v$ resulting in a simple relation for δ_{eon}

$$\delta_{eon}=\sqrt{K_B}\left(\frac{a}{a^*_{eon}}-\frac{a^*_{eon}}{a}\right)=2\sqrt{K_B}\sinh-(\mathcal{E}-\mathcal{E}^*_{eon}) \tag{40}$$

which is isomorphic to Equation (30) with $\mathcal{E}^*$ being replaced by $\mathcal{E}^*_{eon}$.

Similarly for the electronically compensated regime where $C\simeq n$ the analogous relation follows:.

$$\delta_{ion}=\sqrt{K_F}\left(\frac{a}{a^*_{ion}}-\frac{a^*_{ion}}{a}\right)=2\sqrt{K_F}\sinh-(\mathcal{E}-\mathcal{E}^*_{ion}) \tag{41}$$

Hence, it can be concluded that it simplifies the treatment of the theoretical (dis)charge curves if one uses δ_{eon} for a predominant ionic compensation, but δ_{ion} for a predominant electronic compensation.

The defect chemical considerations could of course be driven much further, in particular for the case that the dopant can change valence state. This change can vary the storage capacity significantly, yet a few remarks must suffice. It is well established from high-temperature chemistry that heavy Fe doping of $SrTiO_3$[47] or heavy Pr doping of CeO_2[48] leads to significant variations in both the integral as well as the differential storage capacity. Yet, it is also clear that heavy doping of a binary finally is equivalent to forming a ternary compound.

It has already been mentioned as special features of room-temperature defect chemistry that 1) native defects can be notoriously frozen hence acting as dopants and 2) oppositely charged point defects tend to associate. While the first can be accounted for in the C term, the second phenomenon can lead to significant changes in the defect chemical treatment. Instead of incorporating such effects into the above rather general treatment, only two specific examples will be mentioned. The first is $LiFePO_4$ in which a great portion of

© 2013 Wiley-VCH Verlag GmbH & Co. KGaA, Weinheim

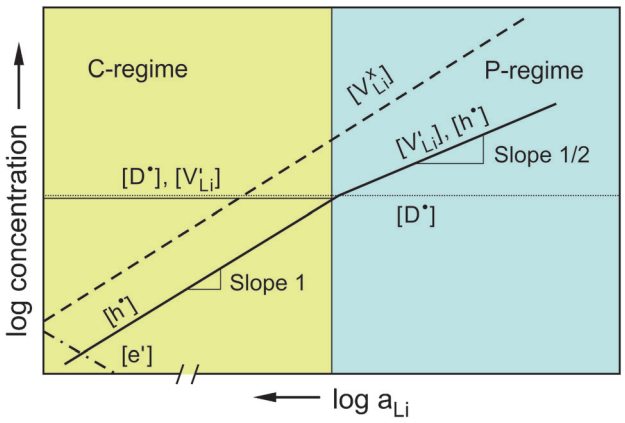

Figure 9. Room-temperature defect chemistry of $LiFePO_4$ as a function of Li activity for a significant Li deficiency.[49] Unlike previous Figures, the association of Li vacancies with holes is taken into account. Note the similarity to Figure 5 (left, red). Reproduced from Ref. [49] with permission from The Electrochemical Society.

the lithium defects (V'_{Li}) appears to be associated with the holes as electronic carriers.

$$V'_{Li} + h^{\bullet} \rightleftharpoons V^{x}_{Li} \quad (42)$$

Atomistically this Equation means that the neighboring Fe ion is in the $+3$ rather than the $+2$ state.

The higher the temperature the more predominant the endothermic dissociation. Figure 9 displays the defect chemistry as a function of Li activity.[49]

The second example is TiO_2 in which, in addition, frozen-in oxygen vacancies play a decisive role for the storage kinetics.[50] Even though frozen, they can exist in various trapped states:

$$V_O^{\bullet\bullet} + 2e' \rightleftharpoons V_O^{\bullet} + e' \rightleftharpoons V_O^{x} \quad (43)$$

The defect chemistry as a function of Li activity is shown in Figure 10. The primary effect of such defect chemical subtleties is their impact on transport properties and hence on the practical performance rather than on the theoretical capacity. Nonetheless, association effects involving lithium defects, such as described by Equation (42) or association of $Li_i^{\bullet}$ with e' occurring in TiO_2 or $FePO_4$, are of significance for storage thermodynamics as this affects the energetic aspects and hence the e.m.f. (see Section 8). The fact that at room temperature such trapping effects are far from being unusual, is reflected by the observation that the introduction of Li often leads to rather modest electronic conductivity modifications.

In the above treatment no competition with other phases was taken into account and hence there was no limit on the a-axis. In reality only a few phases tolerate very large non-stoichiometries. For sufficiently large defect concentrations the molar Gibbs energy will increase to an extent that formation of other phases becomes favorable. This effect gives rise to the bounds δ_{min}, δ_{max} in Figure 6. Even if no competitive phases were of significance (and no limits set by the electrolyte) the finite number of sites to be filled by Li—

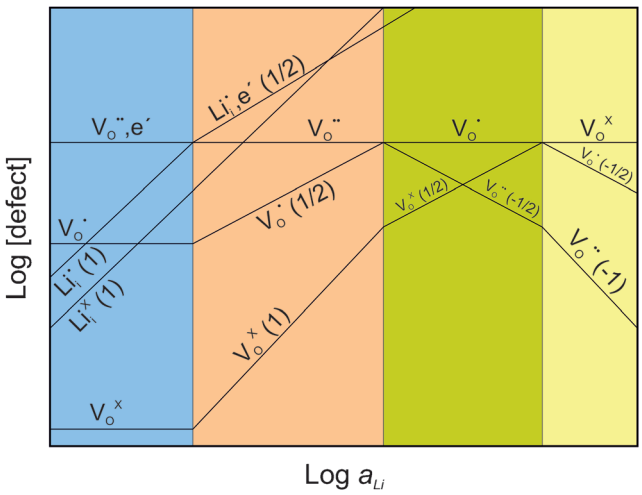

Figure 10. Simplified defect chemistry of TiO_2 at room-temperature as a function of Li activity.[88] Unlike the previous examples the effect of frozen-in oxygen vacancies in various valence states is taken into account (cf. similarity of the situation at low a_{Li} with the situation at high a_{Li} in Figures 5, 7). For simplicity, we suppress the difference between $\log[V_O^{\bullet\bullet}]$ and $\log[e']$ for the cases where $V_O^{\bullet\bullet}$ are the majority carriers. Reproduced from Ref. [50] with permission from Elsevier.

and/or also the finite number of quantum states to be occupied by electrons—would limit storage. In such a general case the Boltzmann distribution used above has to be replaced by the more precise Fermi–Dirac distribution, for example, for the interstitial defect.

$$\mu_i = \text{const} + RT\ln\frac{i}{i_{max} - i} \quad (44)$$

The chemical potential and hence the voltage would diverge for $i \rightarrow i_{max}$. Formally such site restrictions lead to entropy-related activity coefficients (activity coefficient $\equiv a/c$). The same is true if the finite density of states becomes significant for high excess electron or hole concentrations. When using structure elements in the mass-action laws this site restriction follows "automatically".[38,51] If, for example, in the just considered case one takes account of occupied and free interstitial sites separately, then instead of i one uses $[Li_i^{\bullet}]/[V_i]$, with $[V_i] = [Li_i^{\bullet}]_{max} - [Li_i^{\bullet}]$. In other words: one has to employ a Boltzmann distribution in the latter formulation (i.e. the entropic activity coefficients for the structural elements are unity). The effects as a result of these saturation phenomena are indicated in Figure 6 by the dashed lines.

Energy-related activity coefficients express the energetic interactions between defects. Examples are long-range interionic Debye–Hückel type of corrections[52] or corrections based on defect-lattice approximations.[39] We will come back to some of these questions when we discuss how to find high storage materials.

4. Lithium-Storage in Two-Phase Systems

As far as two-phase systems are concerned, we refer to the coexistence of a lithium poor ($Li_{\Theta}X$) with a lithium-rich phase

 © 2013 Wiley-VCH Verlag GmbH & Co. KGaA, Weinheim

($Li_{1-\Delta}X$). At a given temperature and pressure these two coexisting phases pin the chemical potential of lithium in the system under concern if it is binary. If the system is multinary (e.g. $LiFePO_4$, $LiRuO_2$), the non-lithium part can often be considered as invariant under battery conditions (e.g. $X \equiv FePO_4$ or RuO_2), and thus a pseudo-binary treatment is appropriate. In our RuO_2 -example we refer to zone B in Figure 3.

In such a non-variant miscibility gap, neither μ_{Li} nor the individual compositions of the phases vary. When we plot the molar Gibbs energy of mixing as a function of the lithium mole fraction, the compositions of coexistence are determined by the points of tangency of the double tangent as shown in Figure 11 (cf. also Appendix I). The storage is reflected by the variation of the overall value of ξ ("$Li_\xi X$"), which follows from the phase fractions.

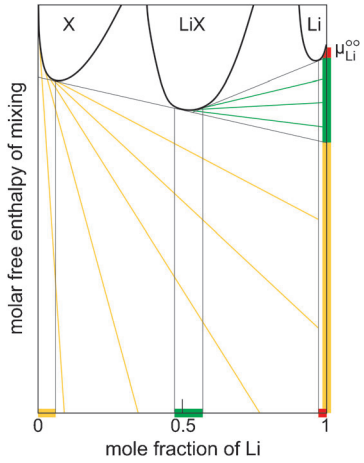

Figure 11. The coexistence concentration in the two-phase fields X:LiX and LiX:Li are determined by the points of double tangency. As the molar Gibbs energy of mixing is plotted (*g*), these double tangents as well as the tangents in the single-phase field (yellow, red, green) intersect the *y*-axis on the right hand side at the respective values of μ_{Li}.

In such pseudo-binary situations an interface is formed and the phase transformation is caused by the lithium content in analogy to temperature- or pressure-driven transformations.

The variation in phase mole fraction x is

$$-\Delta x_\alpha = +\Delta x_\beta = \frac{Q}{F}\frac{1}{n_X}\frac{1}{1-\Theta-\Delta} \tag{45}$$

with n_X being the mole number of X in the phase mixture. Q is the charge transferred, F is Faraday's constant and hence Q/F the mole number of Li transferred. The variation cannot be greater than $|\Delta x| = 1$ and the maximum charge transferred ("storage capacity") is thus simply related to the variation of the Li content in the two phases according to

$$Q_{max} = Fn_X(1-\Theta-\Delta) \tag{46}$$

In principle the cell voltage versus Li can be calculated in the same way as above by using Equation (4). Usually in non-variant cases a more straightforward expression is used [Eq. (50)] that connects with Equation (4) as follows:

Let us denote the Li-poor phase $Li_\Theta X$ by α and the Li-rich phase $Li_{1-\Delta}X$ by β. Unlike the previous case, it is advantageous and common here to relate the cell voltage to chemical phase potentials [Eq. (47)]

$$\mu_{Li_\Theta X}(Li_\Theta X) \equiv \mu_\alpha = G_\alpha/n_\alpha \text{ and } \mu_{Li_{1-\Delta}X}(Li_{1-\Delta}X) \equiv \mu_\beta = G_\beta/n_\beta \tag{47}$$

Owing to additivity of the chemical potentials of the individual constituents the relationship in Equation (48) is valid.

$$\begin{aligned}\mu_\alpha &= \Theta\mu_{Li}(\alpha) + \mu_X(\alpha)\\ \mu_\beta &= (1-\Delta)\mu_{Li}(\beta) + \mu_X(\beta)\end{aligned} \tag{48}$$

Since $\mu_{Li}(\alpha) = \mu_{Li}(\beta)$ (exchange equilibrium) and $\mu_X(\alpha) = \mu_X(\beta)$ (Gibbs–Duhem equation), it follows that

$$\begin{aligned}\mu_{Li} &= \frac{\mu_\beta - \mu_\alpha}{1-\Delta-\Theta} \text{ and}\\ \mu_{Li} - \mu_{Li}^{\circ\circ} &= \frac{\mu_\beta - \mu_\alpha - (1-\Delta-\Theta)\mu_{Li}^{\circ\circ}}{1-\Delta-\Theta}\end{aligned} \tag{49}$$

As $EF = \mu_{Li} - \mu_{Li}^{\circ\circ}$ we recognize that we can express the cell voltage in terms of the cell reaction as

$$z_R EF = -\Delta_R G\{(1-\Theta-\Delta)Li(s) + Li_\Theta X \rightarrow Li_{1-\Delta}X\} \tag{50}$$

with $z_R = (1-\Theta-\Delta)$.

This relation also directly follows from global thermodynamics (chemical work = electrical work). If $\Theta, \Delta \ll 1$, then $z_R \simeq 1$ and the deviation of $\mu_{\alpha,\beta}$ from $\mu_{\alpha,\beta}^\circ = G_{m\alpha,\beta}^\circ$ is small (configurational contributions to the phase potential are of second order) and

$$EF \simeq -\Delta_R G^\circ \tag{51}$$

This Equation is the basis of assessing non-variant cell-voltages from tabulated standard Gibbs-energy values for the phases involved. [As suggested by Eqs. (49), (50) for larger non-stoichiometries, it is clearly a better approximation to take the phase potentials as constant but to take account of the non-integer stoichiometric numbers resulting in non-integer z_R values.]

From a macroscopic thermodynamic point of view the situation in a non-variant multiphase system is not different.[53] So, for example, in the low-voltage regime where $LiRuO_2$ starts decomposing (see zone D in Figure 3) according to

$$LiRuO_2 + 3\,Li(s) \rightarrow 2\,Li_2O + Ru \tag{52}$$

and coexists with Ru and Li_2O, the chemical potential of Li is determined by the local three-phase equilibrium Li_2O:Ru:$LiRuO_2$ and the e.m.f. given by $\Delta_R G^\circ$ of the respective chemical reaction [Eq. (52)]. (But note that, for the thermodynamics to be defined in addition to Li, also O (or Ru) needs to be exchangeable and to exhibit sufficient diffusivity.)

© 2013 Wiley-VCH Verlag GmbH & Co. KGaA, Weinheim

An excellent measure of the equilibrium voltage of such systems is the equilibrium oxygen partial pressure defined by such systems. For ternary systems of the form Li_vMO_w:Li_xMO_y:Li_2O such as $LiRuO_2$ ($v=1$, $w=2$): Ru ($x=y=0$):Li_2O the connection between cell voltage and oxygenation power (μ_O) is readily demonstrated. Both μ_{Li} and μ_O (as well as μ_M) depend very sensitively on the fine composition (e.g. of Li_2O). Yet in the above multi-phase mixture of the ternaries all these fine compositions and hence chemical potentials are well defined (Gibbs' phase rule). As for the common Li_2O μ_{Li} and μ_O are coupled according to $2\mu_{Li}+\mu_O \simeq \mu^{\circ}_{Li_2O}$, one obtains a linear relation between cell voltage and log (equilibrium oxygen partial pressure) = const. $+2\mu_O$ as demonstrated in Ref. [54] for such composites.

Unlike in the two-phase situation, such conversion reactions lead to a greater morphological complexity. It turns out for the example just given that the phase distribution is heterogeneous even on a nanoscale. This is an expression of the low diffusivities of O and Ru at room-temperature and simultaneously a prerequisite of achieving a certain reversibility. Hence such nanostructural morphology may be conceived as an expression of the "reaction–diffusion domains" developed.

5. Excursion: Thermodynamic Aspects of Nanocrystalline and Amorphous Materials

Even though variations in E and δ are not the primary causes for using nanocrystals, these quantities are also measurably influenced by size. This needs to be addressed not only as nanostructures may be automatically generated through conversion reactions, but in particular since nanocrystals are deliberately used in the single or two-phase modes. Nanocrystallinity is not the only phase metastability[55] of significance in the battery context, also amorphous phases frequently occur. To treat such metastable situations as constrained equilibrium states one has to make sure that the exchange processes that are necessary for the property to be investigated (e.g. Li exchange for e.m.f.) are reversible (while immobile counter elements, that is, X in LiX, maintain the frozen-in structure).

Absolute values and signs of the voltage variations depend on whether single- or multi-phase mechanisms are relevant.

For a more reliable treatment of the thermodynamics of nanosized particles, the reader is referred to the literature.[6,56–60] It suffices to mention that the situation is particularly complicated if surface stress effects[57,61] come into play, or deviations from the equilibrium shape at a given size or the size dependencies of surface and bulk energies have to be involved.

Herein we concentrate on ideal Wulff-shaped crystallites, neglect surface stress effects,[62] and assume the excess free energies of the individual surface planes (orientation (s)) over the bulk value to be determined by size-independent surface tensions (γ_s). The Wulff-shape which is the equilibrium shape[63] for the addressed idealizations, is characterized by γ_s/h_s values which are independent of s, where h_s denotes the distance of the plane with orientation s from the origin. In other words

$$\gamma_s/h_s = w = \langle\gamma\rangle/\langle h\rangle \tag{53}$$

where w is a constant with respect to s. The ratio w can also be favorably expressed in terms of the area averaged mean values ($\langle\gamma\rangle = \Sigma_s a_s \gamma_s/\Sigma a_s$, $\langle h\rangle = \Sigma_s a_s h_s/\Sigma_s a_s$; the a_s values are the areas of the crystal faces of the Wulff crystal; its volume being $\Sigma_s h_s a_s/3 = \langle h\rangle \Sigma_s a_s/3$).[59]

The surface effects lead to an enhanced pressure given by $2w$ (more precisely, the normal, not tangential, pressure is decisive for the volume work term while the difference between normal and tangential pressure is relevant for the surface work term because it enters into the calculation of γ).[56,57] As a consequence of this capillary pressure, the chemical potentials are varied. This is of importance on the phase level (1), the component level (2), and the defect level (3).

1) The chemical potential of the crystallite is increased by $2vw$ (v: molar volume of the phase), 2) the chemical potential of a component k by $2v_k w$ (v_k: partial molar volume of the component, for example, Li in LiX), and last but not least 3) the chemical potential of a point defect d by $2v_d w$ (v_d: partial molar volume of the defect).[64] Unlike v, the partial molar volumes v_k and v_d can be negative.[56,57] (Appendix II gives the connections between the chemical potentials on the different levels.)

The most well-known phenomenon in nanoscience related to point (1) is the much lower melting point[65] of nanocrystals compared to macroscopic single crystals (Appendix IV). Examples for the variation on the component level (point (2)) are varied Li activities for different sizes and hence varied cell potentials. This effect is impressively demonstrated in quasi-symmetrical cells where the right-hand side (RHS) and left-hand side (LHS) of the cell only differ in particle size but this still leads to non-zero e.m.f.[66–68] The capillary effect on the defects (point (3)) results in a varied defect chemistry by varied defect-chemical mass-action constants. If we concentrate on the capillary effects, the mass-action constants that depend exponentially on the standard potential, obviously change with size r according to

$$\frac{K(r)}{K(r=\infty)} = \exp\left(-2\frac{\Delta_R(vw)}{RT}\right) \tag{54}$$

where the right-hand side term refers to variations of partial molar volume, size, and surface tension during the reaction.[64]

If we refer to Li storage we phenomenologically concentrate on the component level, but mechanistically on the defect level as both are naturally interconnected (Appendix II). Given usual γ values, the capillary term is typically small if the 10 nm size is exceeded; but for interfacial distances below 10 nm the impact may be significant. However, it must be noted that preparations of differently sized particles usually imply variation in surface chemistry (γ) as well as volume effects (v). This is demonstrated by recent results on $LiFePO_4$.[69]

© 2013 Wiley-VCH Verlag GmbH & Co. KGaA, Weinheim

With γ values between 0.1 to 1 $J\,m^{-2}$, $|v|$-values between 0 and 3×10^{-5} $m^3\,mol^{-1}$, and sizes between 5 and 50 nm it is clear that excess e.m.f. values are expected not to exceed ±100 mV.

For the following considerations it is appropriate to distinguish between the Gibbs energy of a mixture per total number of moles (n_X+n_{Li}) and the Gibbs energy of a mixture per mole number of the invariant component (n_X for $Li_\xi X$). The first we denote as g, the second as Γ (cf. Appendix I).

Figure 12 refers to the molar Gibbs energy $g(x)$ of mixing (Li and X) of a metastable LiX (nanosized, amorphous) for a single-phase storage. The fact that the g curve is increased compared with the stable LiX situation does not necessarily lead to increased chemical potentials of lithium, reflected by the intercept at the $x=1$ axis of the tangent at x (see also Appendix I). This is however definitely the case if the shape of the $g(x)$ curves is preserved (i.e. they are shifted by Δ with $d\Delta/dx_{Li}=0$). The justification of such an assumption will be inspected below (see Figure 12, top). Because of the thermodynamic relation

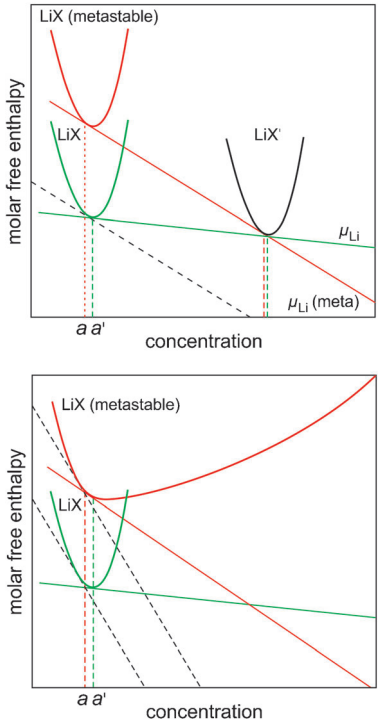

Figure 12. Top: If only the Li-poor phase has a metastable variant and if for simplicity the excess Li value is independent of concentration, the Li potential for the metastable phase is smaller than for the stable one in the two-phase regime ($a<x_{Li}<b$; see green and red tangents) but greater in the single-phase regime, if $x_{Li}<a'$ (see black tangents). The transition occurs between a' and a in contrast to the single-phase situation (dotted line) or in the case (not shown) that the Li-rich phase is the metastable one. If the y-axis refers to g, then the concentration variable is x_{Li}. If it refers to Γ then the concentration variable is ξ. In the first case the chemical potential of lithium is the intercept at $x_{Li}=1$, and the approximation of a constant excess value is good for $v_{Li}=v_{LiX}/2$ in the case of capillarity. In the second case μ_{Li} is the slope, and the approximation of the constant excess value is good for $v_{Li}\ll v_{LiX}$. Reproduced from Ref. [71] with permission from The Royal Society of Chemistry. Bottom: A situation is shown where the form of the g (x_{Li}) curve or $\Gamma(\xi_{Li})$ curve leads to an inversion within the single-phase storage mode.

$$\mu_{Li}=g+(1-x_{Li})\frac{dg}{dx_{Li}} \tag{55}$$

where x_{Li} is the Li mole fraction in $Li_\xi X$ ($x=\frac{\xi}{1+\xi}$) (cf. Appendix II) this means for the excess values (difference of the values for small and large r($r=\infty$)) that $\mu_{Li}^{ex}=g^{ex}$, that is, $dg^{ex}/dx_{Li}=0$. Then the tangents at x_{Li} for $g(r)$ and $g(\infty)$ are parallel and the intercepts of the tangents with the axis $x_{Li}=1$ are shifted in the same way. In such a situation the capillary effect lowers the distance to the reference value of elemental Li, which has the highest μ_{Li} value, and thus lowers the cell voltage. Even though the assumption of a constant Δ may give an intuitive insight, for the capillary effects in LiX it is quantitatively only correct if $v_{Li}=\frac{v_{LiX}}{2}$ (Appendix I). Then the Li "feels" the full capillary effect. For the opposite case, that v_{Li} is negligible compared with v_{LiX}, not Δ but Δ' is constant, which is the distance between the curves in the $\Gamma(\xi)$ representation (cf. Appendices I, III). As here the chemical potentials are the slopes, μ_{Li}^{ex} vanishes. As generally $\mu_{Li}^{ex}=\frac{2\gamma}{r}v_{Li}$, the truth lies somewhere is in between.

Owing to the importance of this point, it is useful to consider the explicit example of single-phase storage in $Li_{1+\delta}X$ in the N regime ($\delta=i=n$). Then according to Appendix II:

$$\begin{aligned} g^{ex}_{Li_{1+\delta}X}&\simeq\frac{2\gamma}{r}\left[\frac{v_{LiX}}{2+\delta}+\frac{\delta}{2+\delta}(v_i+v_n)\right]\\ &=\frac{2\gamma}{r}[(1-x_{Li})v_{LiX}+(2x_{Li}-1)(v_i+v_n)]\end{aligned} \tag{56}$$

in a simpler form for Γ^{ex}

$$\Gamma^{ex}_{Li_{1+\delta}X}\simeq\frac{2\gamma}{r}[v_{LiX}+\delta(v_i+v_n)]=\frac{2\gamma}{r}[v_{LiX}+(\xi-1)(v_i+v_n)] \tag{57}$$

The relation $\mu_{Li}^{ex}=\frac{2\gamma}{r}(v_i+v_n)=\frac{2\gamma}{r}v_{Li}$ consistently follows from both equations through:

$$\mu_{Li}^{ex}=g^{ex}+(1-x_{Li})dg^{ex}/dx_{Li}=d\Gamma^{ex}/d\xi.$$

The shift in the respective free-energy curve involves v_{LiX} (shift at $\delta=0$) as well as $v_{Li}=v_i+v_n$.

The upwards shift in μ_{Li} corresponds to a lowering in the e.m.f. (vs. Li) as for example, shown by recent results on nanocrystalline $LiFePO_4$.[69] Here $v_{Li}\simeq10\%$ v_{LiX} and the excess voltages are in fact expected to be significantly smaller than expected from Figure 12.

In the two-phase storage mode, the calculation of the e.m.f. effect is more straightforward, as in this case according to Equation (51) the e.m.f. (i.e. μ_{Li}) is directly given by the μ values of the phases involved (which are approximately equal to the μ° values).

The e.m.f. effect is not very pronounced in the two-phase system if both phases in contact are affected by the capillary effect in a similar way. In such a case $\Delta(2\gamma v/r)$ is relevant though this term might be small. The magnitude of the effect depends on the phase-change mechanism. In a core–shell mechanism, γ of the core is determined by the possibly small interfacial tension, while γ of the shell is greatly influenced by the typically greater surface contribution. The effect can be

© 2013 Wiley-VCH Verlag GmbH & Co. KGaA, Weinheim

particularly pronounced if only one phase is metastable (see Figure 12). As mentioned in the beginning,[17] in RuO_2 massive lithiation eventually leads to an extremely fine mixture of Li_2O and Ru, which can be delithiated again to form amorphous RuO_2. On mild lithiation this RuO_2, if saturated with Li, transforms into $LiRuO_2$ which is now crystalline. Hence one expects significant e.m.f. variations even though the observed magnitude greatly exceeded the expectations.[70,71] The open-circuit voltage measured in this situation was found to be enhanced by as much as 500 mV with respect to the macroscopic RuO_2:$LiRuO_2$ two-phase mixture. Two points are remarkable here: 1) the very large excess value and 2) the fact that this excess value is positive. The latter point becomes clear when Figure 12 is considered and arises because in our example it is the Li-poor phase which is metastable, while the Li-rich phase is stable. The decrease of μ_{Li} below the macrocrystalline value reflects the variation in Gibbs energy being more favorable if the crystalline $LiRuO_2$ is formed from the metastable RuO_2 than from the stable RuO_2.

The analysis based on Equation (55) has led to a far-reaching interpretation of these RuO_2 results. Even indications of the expected reversal of the sign of the excess e.m.f. when crossing the border between two-phase and single-phase mode, have been indicated.[72]

The other intriguing aspect is that the value of 500 mV is much larger than the usual excess values for nanocrystalline particles. Such a value would be formally expected for unrealistic crystallites of atomistic size. Indeed it turned out that whenever such high values were observed, the RuO_2 was amorphous. Thus, the value follows directly by connecting it with the loss of long-range order and hence explaining it through the free melting enthalpy at room temperature. For details see Refs. [70,71]. In these references and Appendix IV it is set out, though, that both ways of interpretation (amorphous and sub-nanocrystalline aggregates) are in a very rough approximation essentially identical as far as the energy aspect is concerned. The interpretation finally relies on the simple argument that interfacial atoms in nanocrystalline materials can be viewed as having lost long-range order. (Here, it is tacitly assumed that the short-range order is unaltered. Consider $LiFePO_4$ for a counter-example.)[69] The simultaneous validity of the two rules of thumb, namely that 1) the excess energy of an amorphous material may be identified with the melting free enthalpy at operational temperature and 2) that it can be understood by the extreme of a capillary effect, implies the validity of a remarkable relationship between γ and melting enthalpy $\Delta_m H_{LiX}$, namely

$$\gamma \sim \frac{\Delta_m H_{LiX} r_0}{2v} \tag{58}$$

with $r_0 \approx 1$–10 Å and v being the molar volume of the compound. One must however note that these rules of thumb are orders-of-magnitude considerations and have to be taken with at least one pinch of salt. Of the same roughness (though helpful) is the implication that r_0 can be identified with the particle radius that is necessary to reduce the melting point down to 0 K by capillarity (see Appendix IV).

For a more reliable interpretation again the defect chemical analysis is decisive (for more details see Appendix I, II, III).

The above correlation is only straightforward for two-phase storage. Only in this case is μ_{Li}^{ex}, as discussed above, directly related to $\mu_{LiX}^{\circ ex}$ which can be correlated with the molar Gibbs energy of melting, $\mu_{LiX}^{\circ ex} \simeq \Delta_m G_{LiX}$ [see Eqs. (50), (51)]. This result is naturally also obtained from Equation (55) if dg/dx_{Li} is replaced by the slope of the double tangent.[70,71]

As for nanocrystalline materials, the treatment of the amorphous state is more complex in the single-phase regime. If we simply ignore dg/dx_{Li} (i.e. assuming a constant shift in the $g(x)$ representation) we would obtain $\mu_{Li}^{ex} = g_{LiX}^{ex} = \Delta_m G_{LiX}/2$. More generally $v_{Li} \neq v_{LiX}/2$ and by naively correcting the above results as done in the single phase situation, we would get:

$$\mu_{Li}^{ex} = \frac{2\gamma}{r_0} v_{LiX}\left(\frac{v_{Li}}{v_{LiX}}\right) = \Delta_m G_{LiX}\left(\frac{v_{Li}}{v_{LiX}}\right).$$

As however the role of the defects is very different for amorphous and crystalline states, none of these approaches is satisfactory. The situation is clearer if we consider the identity $\Gamma^{ex} = \mu_{LiX}^{\circ ex} + \delta\mu_{Li}^{ex}$. Assessing the first term (which describes the situation for $\delta = 0$) by $\frac{2\gamma}{r_0} v_{LiX}$ or by the Gibbs energy of melting, may be an acceptable approximation. Yet, using a similar approximation for the second term describing defect formation and being the relevant term for the e.m.f., could be grossly wrong. Defect formation in the arrangement of clusters without long-range order is very different from the nanocrystalline state. Vacancies and interstitials may be very favorably formed at spots where they can release the inhomogeneity stress, so that the formation free energies of the ionic point defects may be distinctly lower.[73] On the other hand electronic defects might be accommodated less easily than in the crystalline state making even the sign of μ_{Li}^{ex} unclear. A typical $\mathcal{E}$ versus δ curve of amorphous materials assumes a smeared-out character: flatter appearance within the homogeneity range of the crystalline phase combined with an extended miscibility. (The behavior is close to the situation investigated in Section 8, cf. Figure 23 there). Apart from kinetic effects this can be ascribed to: 1) Flattening as a result of easier Li incorporation (higher K_{Li} in the N regime, cf. Figures 19, 23 in Section 8); then however $\mathcal{E}$ must be increased compared to the crystalline situation; 2) Favorable interactions, such as $Li_i^{\bullet} + e' \rightleftharpoons Li_i^{x}$, in the N regime. A dominant effect would lead to an equation similar to Equation (31) but without factor 2. 3) Natural flattening for larger δ [Eq. (31)], should competing phases become less relevant.

A shrunk miscibility gap has also been observed for nanocrystalline materials. This can hardly be explained by capillarity only. Defect concentrations are expected to be comparatively small [cf. Eq. (54)]. Concentrating for example, on the N regime in $FePO_4$ the μ° values of i and n would rather increase and K_{Li} decrease which is in contrast to the observation that the miscibility range is extended. Increased miscibility can, for example, be attributed to the cost of interface formation which is not negligible at small size.[74–77]

© 2013 Wiley-VCH Verlag GmbH & Co. KGaA, Weinheim

This penalty can be significantly altered if gradient effects are included. The corresponding Cahn–Hilliard correction favors graded interfaces. (Recent TEM results[78,79] even indicated staging effects at interfaces and in nano samples.

Even within the miscibility gap, the voltage–composition profile is usually no longer horizontal for nanocrystals. One reason is the unavoidable distribution of size, shape, and surface chemistry (distribution of w within a nanocrystalline ensemble).[80]

There is an even more fundamental aspect to be mentioned which, however, is restricted to extremely small sizes:[81] In such extreme cases, the chemical potential of an individual nanoparticle experiences a contribution from the particles' configurational entropy. In such cases the nanoparticles behave as an intermediate between extended solids and atomic particles, and one has to reckon with different charge carrier densities from particle to particle, even if they are identical in structure, shape, and size.

At very tiny size the standard potentials[81] are expected to not only vary through capillarity but also because of energetic confinement of the point defects, a well-established effect for electronic defects.

A size effect that can become relevant for nanoparticles with larger radii concerns the configurational entropy of defects, it occurs in nanocrystals in which the space-charge zones overlap and cover the entire crystallite.[82]

Evidently, the thermodynamics at the nanoregime offers a variety of challenges and a range of properties, connected with Li batteries, which are far from being clarified.

6. Interfacial Storage and "Job Sharing"

Higher-dimensional defects can lead to additional Li storage if special sites are available, and the site occupation is not too costly energetically $(\mu_{Li} < \mu^{\circ\circ}_{Li})$. The equilibrium distribution between lattice sites in the core of the interface (where the sites have a different energy to that in the bulk phase) and bulk sites can be calculated through Equation (59)

$$\mu^{\circ}_{Li}(\text{bulk}) + RT \ln a_{Li}(\text{bulk}) = \mu^{\circ}_{Li}(\text{core}) + RT \ln a_{Li}(\text{core}) \quad (59)$$

Core storage of neutral lithium is the consequence of the altered structure which leads to a difference in the μ°_{Li} values. A core storage can also be connected with an excess charge, so for example, Li^+ can accumulate in grain boundary cores while the electron clouds extend into the neighboring crystal regions (or vice versa). Such excess storage can also be discussed for Li storage at dislocation cores or in frozen vacancies, such as in carbonaceous materials.[23]

While all this is not conceptually different from storage in a metastable 3D structure, the contact of two phases allows for a novel interesting storage mode that is based solely on the formation of a space-charge storage zone and will be in the focus of the rest of the this Section.

This mode may culminate in the striking peculiarity that the contact alone (no excess storage in interfacial core) of two phases, neither which none is able to store Li, can result in Li storage nonetheless ("*job-sharing" mechanism*).[20,21] Consider for example, the contact of Li_2O and Ru. It is known that both phases do not store Li to a noteworthy amount, because Li_2O cannot accommodate the electrons while Ru clearly does not accommodate Li^+. However the nanoscopic mixture of both does store lithium to a significant degree (cf. region E in Figure 3).

The reasoning is simple: Ru as a noble metal can easily take up electrons in the outmost layer, while Li_2O can, owing to the antifluorite structure, easily accommodate excess lithium ions (Figure 13).[20,21] The same phenomenon may be

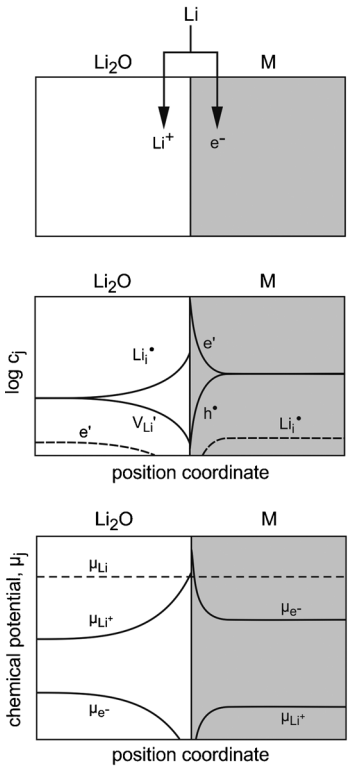

Figure 13. Mechanism, defect concentrations, and chemical potentials at a "job-sharing" contact. Reproduced from Ref. [22] with permission from The Royal Society of Chemistry.

observed in other conversion-reaction products or for deliberately fabricated two-phase contacts. Shrinking, in a thought experiment, the size of the phases to atomistic size one easily realizes that this storage mode forms the link between an electrostatic and a chemical capacitor.

Figure 13 shows the thermodynamic situation, whereby for the purpose of a thermodynamic definition, we allow for a minute e^- accommodation in Li_2O and a minute Li^+ accommodation in Ru. Clearly storage of Li is realized even though the μ°_{Li} values (in the given phase) as well as the μ_{Li} value are invariant. This is the consequence of the heterogeneity of the process, that is, Equation (60).

$$\text{"Li"} = Li^+(\alpha) + e^-(\beta) \quad (60)$$

The well-established underpotential deposition of Li caused by adsorption of Li^+ out of the electrolyte to the electrode

 © 2013 Wiley-VCH Verlag GmbH & Co. KGaA, Weinheim

(while the e^- is stabilized by the electrode) can be considered as a subcase.

Another very relevant special case is possible storage in the solid–electrolyte interface (SEI),[83,84] the passivation layer that forms at electrode/electrolyte contacts at very low or high potentials. This SEI is a thin ion-conducting, but electron-blocking passivation layer guaranteeing the kinetic stabilities of many electrode/electrolyte contacts. Besides irreversible Li storage in the SEI (which is equivalent to irreversible passivation reactions), solubility of Li^+ in the SEI (for which we approximately take the composition of Li_2O), compensated by e^- in the electrode (or current collector), is possible. Note that a significant accommodation of both Li^+ and e^- in a passivating stationary SEI is improbable, as it would make it mixed conducting (or at least Li permeable) resulting in further growth of the SEI layer.

In the following it is useful to compare bulk and job-sharing interfacial mechanisms with regard to size and voltage dependencies. For a detailed calculation of the relevant defect chemistry in such a space-charge-controlled case see Ref. [22]. Let us for simplicity consider a heterolayer arrangement (see Figure 14) and vary the thickness L. Clearly for bulk storage, the stored mass Q is proportional to L. In

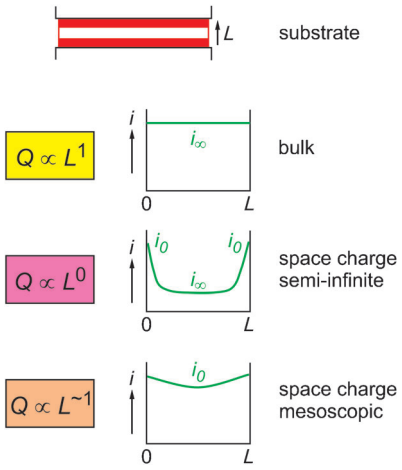

Figure 14. Thickness depends of space–charge storage capacity for thin (center) or very thin (bottom) layers as compared with the bulk storage (top).

contrast, the storage in the semi-infinite space-charge zones (i.e. space-charge zones do not cover the whole layer) is independent of L, while in the mesoscopic situation where space-charge zones overlap, the situation again develops towards a proportionality to L.

More revealing is the dependence on $\mathcal{E}$ or a_{Li}. Let us for simplicity just consider interstitial storage and assume that there is inexhaustible supply of available sites and no interaction effects. (Extensions may be more complex but straightforward.)

Recalling, how we calculated the mass stored Q (or δ) in the bulk [Eq. (31)], we first consider the homogeneous reaction (cf. N regime in Figure 4–8).

$$Li + V_i \rightleftharpoons Li_i^\bullet + e' \tag{61}$$

Owing to electroneutrality, $[Li_i^\bullet] = [e']$, and it follows that

$$Q \propto [Li_i^\bullet] \propto a_{Li}^{1/2} \tag{62}$$

In the heterogeneous situation we have to formulate

$$Li \rightleftharpoons Li_i^\bullet(\alpha) + e'(\beta) \tag{63}$$

where, at the moment, we do not need to specify which position in the space-charge zone we refer to. The balance of the chemical potentials that led to mass–action laws has to be replaced by the balance of the electrochemical potentials. The heterogeneity gives rise to two characteristic features: 1) The mass–action constant (K_{het}) is composed of the μ_i° value of phase α and the μ_n° value of phase β. 2) Furthermore, the mass–action constant has to be corrected by the electrical-potential drop between these two distant sites, which depends on the concentrations again. (The whole problem can be solved by involving Poisson's equation leading to Gouy–Chapman or Mott–Schottky profiles.) This potential drop includes the potential drop in phase α going from its bulk to the outermost layer adjacent to the neighboring phase β, the potential drop from there to the outermost first layer of the neighboring phase β, and then the drop from there into the bulk of phase β.

We best approach the problem by referring in Equation (63) to the outermost layers in each phase (denoted by α, 0 and β, 0) forming the abrupt transition, as they limit the space-charge profiles. The application of the balance of the electrochemical potentials to Equation (63) leads to

$$[Li^\bullet(\alpha,0)][e'(\beta,0)] = K_{het}\kappa a_{Li} \tag{64}$$

with K_{het} being the mass–action constant of Equation (63); $\kappa = \exp\left(-F\frac{\phi(\alpha,0)-\phi(\beta,0)}{RT}\right)$ is determined by the electrical potential drop between α, 0 and β, 0.

From these outermost layers the concentrations decay into the respective bulk regions. We arrive at a simple solution, if we can ignore the potential drop between the outermost layers, corresponding to an atomistically small contact distance, that is, by setting $\kappa = 1$. This approximation is referred to in Figure 15. The integral of the Gouy–Chapman profiles thus formed on either side, corresponds to the total charge. Naturally these integrals have to be different in sign but equal in magnitude. The overall charge turns out to be proportional to the square root of the above boundary concentrations as well as to the dielectric numbers ε_α, ε_β.[85] Hence, the boundary concentrations are proportional to each other, yielding

$$Q \propto [Li^\bullet(\alpha,0)]^{1/2} \propto a_{Li}^{1/4} \tag{65}$$

a result quite different from Equation (62). (The constant of proportionality is given by $\sqrt{2\varepsilon_\alpha RT}$ times area.)

Further size reduction to an extent that the space-charge zones strongly overlap and the values of $Li^\bullet(\alpha,0)$, $e'(\beta,0)$ tend

© 2013 Wiley-VCH Verlag GmbH & Co. KGaA, Weinheim

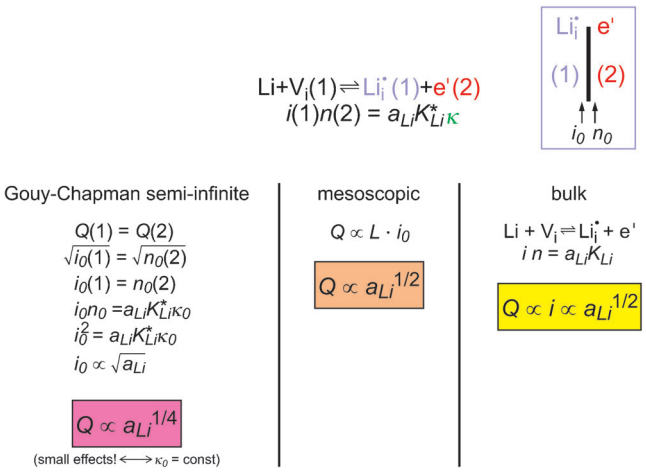

Figure 15. Activity dependence of the job-sharing capacity for thin (left) and very thin (center) layers as compared with bulk storage as long as the electrical potential drop over the core region can be ignored. Note that here *i*, *n*, *K* refer to molar concentrations.

to be realized everywhere in α or β, leads back to a $a^{1/2}$ dependence [Eq. (66)].

$$Q \rightarrow \text{prop. } a_{\text{Li}}^{1/2} \tag{66}$$

In this limit the composite behaves as a pseudo-single phase. The comparison between Equation (62) and Equation (65) shows that

$$Q_{\text{scl}}/Q_{\text{bulk}} \propto a_{\text{Li}}^{-1/4} \tag{67}$$

which emphasizes that bulk and space-charge storage occur simultaneously with the space-charge contribution becoming less pronounced compared to the bulk contribution for higher lithium activities (lower e.m.f.). This situation is not in contrast to the fact that the interfacial storage only occurs in the conversion reaction at very low voltage (cf. Figure 3, region E). The reason is that in these examples, phases with active interfaces are only formed at low voltage while the respective bulk phases present at higher voltages are inactive.

Complementing the above, it must be stated that it is not justified to neglect the potential drop at the contact in spite of the small distance (*s*). The sensitivity of this region is obvious from the following consideration. If one assumes a charge-carrier-free zone, the potential evolution is linear between (α, 0) and (β, 0) but with the same extreme slope that is realized at (α, 0) or (β, 0). This potential drop[86] is given by $\frac{s}{\varepsilon_T}\sqrt{2\varepsilon RTi_0}$ (ε_T: dielectric constant of that region) if for simplicity *i* and *K* (unlike previously) refer to molar concentrations. If we set $s \simeq 0.5$ nm, $\varepsilon_T \simeq \varepsilon_\alpha = 10\,\varepsilon_o$, then for $i_0 \simeq (1/30)$ mol cm^{-3}, the voltage drop is about 1 V which greatly exceeds *RT*/*F*.

Even though the identification of ε_T with ε_α or ε_β can be considered as an upper limit, κ is far from being unity. Taking this into consideration, one finds:

$$a_{\text{Li}} = K_{\text{het}}^{-1} i_0^2 \exp\left[\frac{Fs\sqrt{2\varepsilon RTi_0}}{RT\varepsilon_T}\right] \propto Q^4 \exp(\text{const}\,Q) \propto \exp -\mathcal{E} \tag{68}$$

High storage clearly favors the exponential term which, if dominant, corresponds to a proportionality between $\mathcal{E}$ and *Q*, as expected for a classical electrostatic storage. Low storage corresponds to the proper diffuse space-charge storage ($\mathcal{E} \propto p + q\ln Q$). The shape predicted is quite similar to zone E in Figure 3. The fact that rather linear parts in the $\mathcal{E}(Q)$ curves are characteristic features in the experimental studies of interfacial storage signifies the importance of the potential drop.

If the particles sizes shrink towards atomistic dimensions the exponential term is to be replaced by unity and the power of $^1/_4$ by $^1/_2$ (see Figure 15) yielding the bulk-like response of this virtual phase.

It is to be expected that the future exploration of the job-sharing mechanism will yield exciting information beyond the pure battery aspects. In terms of potential applications it is the beneficial compromise between power and energy density that stands out.

7. A Few Remarks with Respect to Non-Equilibrium: The Significance of Point-Defect Chemistry and Morphology

In this Section we briefly consider the situation under current flow for three reasons:

1) Strictly speaking thermodynamics does not exclusively concentrate on equilibrium (thermostatics) but also deals with rate vs. driving force relations (irreversible thermodynamics). This is particularly the case in the range of linear irreversible thermodynamics for which we can consider the relevant resistances and capacitances as equilibrium quantities (in the sense of the first non-constant term in a Taylor expansion of rate in terms of driving force).
2) The defect-chemistry considered above is not only important for understanding equilibrium storage, but also for kinetic phenomena, such as diffusion rates, migration rates, transfer rates, or reaction rates.
3) Reaching equilibrium at room temperature is not trivial and dealing with a few characteristic kinetic features helpful.

Outside equilibrium the situation necessarily becomes very specific and that is why a few remarks must suffice. For more details the reader is referred to the literature.[29]

As far as global energetics is concerned, one can state, that non-equilibrium implies non-zero (but of course positive) entropy-production $\delta_{\text{int}} S$.

For constant *p*, *T*

$$-T\delta_{\text{int}}\,S = d\tilde{G} < 0 \tag{69}$$

where $d\tilde{G}$ is the change in the total Gibbs function also including electrical work terms. The entropy production can be written as the product of fluxes and overvoltages.[87] Overvoltages mean a lower efficiency and non-zero dissipation that can be recast in terms of resistances *R* (diffusion resistance, transfer resistance, reaction resistance etc.) leading

© 2013 Wiley-VCH Verlag GmbH & Co. KGaA, Weinheim

for a non-zero current I to a voltage that differs from E according to

$$U(I) = E + \Sigma_i I R_i \tag{70}$$

At a great distance from equilibrium, a situation easily attained for reaction resistances, the R_i values become current dependent. For the charging process we define the current as positive, hence $U > E$, while during discharge the current is negative and $U < E$. Losses owing to resistances can have many causes, such as sluggish electrochemical reaction kinetics, slow transport kinetics in the electrolyte, concentration polarization in the electrolyte, polarizations connected with the passivation layer, contact difficulties in the electrode network, nucleation, and most importantly transport problems in the electrodes.

The last point is indeed in many cases the relevant one. As far as such transport effects are concerned, it is primarily the optimization of charge-carrier chemistry that is required. The classic adjusting screws are doping, component partial pressures, and temperature. If we can assume that all the components but Li are frozen, then the parameters remaining are dopant concentration, the component partial pressure, and the temperature of preparation. In Section 3 we, for example, considered the effect of frozen-in oxygen stoichiometry in TiO_2 on the defect chemical situation at room-temperature.[50,88] One has to note, however, that wherever the decisive ionic Li defect (e.g. $Li_i^{\bullet}$ in TiO_2) and electronic defect (e.g. e' in TiO_2) are oppositely charged (as expected for large storage effects) the effect of doping—even though possibly not insignificant—is not expected to be exceedingly high as the impact on bulk concentration is of the opposite nature. Also heterogeneous doping or more generally the introduction of interfaces proved to be of high significance for defect chemistry.[81] The splitting of concentration profiles leads to the same counteracting behavior of oppositely charged carriers. But here the heterogeneity may be favorably used in a layered configuration: for example, through enhanced ionic transport in the boundary while electron transport chiefly occurs in the bulk. The relevance of this technique for electrode kinetics is yet to be explored. At any rate, this counteracting behavior is extremely beneficial for electrolytes, in which accumulation of Li^+ accompanied by depletion of counterion is desired. We briefly come back to this point in the context of Soggy Sand Electrolytes[89] (see Section 8).

If all the possibilities to improve the transport coefficients are exhausted, decreasing the diffusion length is still a straight-forward parameter to play with. This is the major reason why one intends to make the electrode particles nanocrystalline. Since usual lithium diffusion coefficients in solids are indeed small at room-temperature and cannot be greatly increased, down-sizing is the remaining remedy as the diffusion time is proportional to $D_{Li}/(\text{particle size})^2$. Storage times that would be on the order of years for 1 mm thick particles shrink to much less than a second if one reduces the size to the nanoregime. Yet this effect can only be exploited if both e^- and Li^+ are quickly transported to the innumerable tiny particles (or active interfaces). Easy Li^+ access is enabled by using a liquid electrolyte and preferably a hierarchical channel structure. The electron access is guaranteed if electrode particles are made of a very good electron conductor, such as graphite. Promising materials, such as $LiFePO_4$ or TiO_2, are however quite insulating and the addition of carbon as an electronic connector is required.

Figure 16 indicates much more powerful network solutions for different dimensionalities, as far as nanostructuring is concerned, that implement ionic and electronic wiring down to the nanoscale.[90–93] As further representatives of various literature examples, the morphologies designed in Refs. [94–99] are be mentioned here.

As far as practical performance is concerned, often simply the volume change during storage prevents a good performance.[94] A very instructive example is Sn, which in principle can dissolve a lot of Li but is useless in compact form for that very reason. The nanostructure shown in Figure 17 however provides an instructive solution hitting various birds with one stone:[92,93]

1) The size of the particles is small enough to guarantee quick Li dissolution/exsolution. 2) The carbon acts an electron connector. 3) The Li^+ ions are brought by the electrolyte to the large surfaces of carbon and can also migrate in the

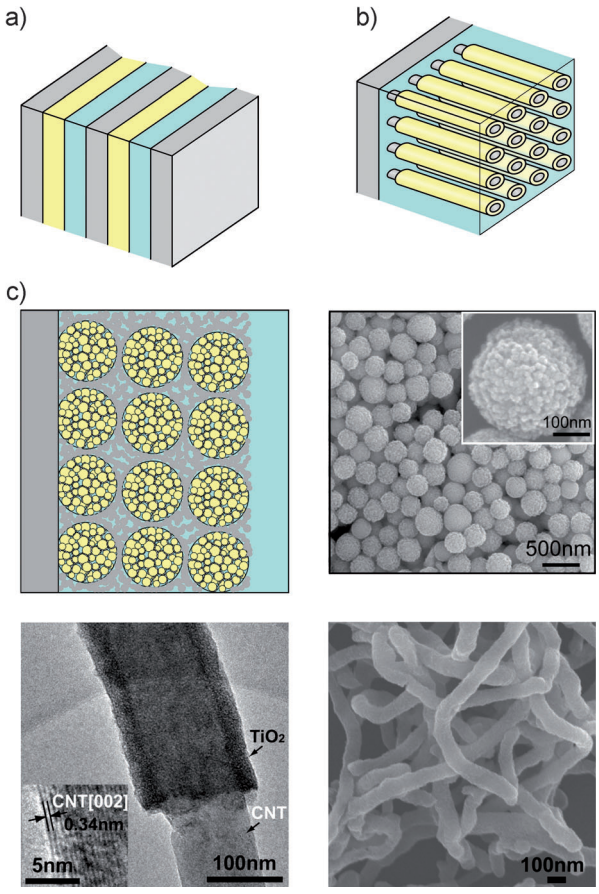

Figure 16. Solutions for effectively mixed conducting networks (see text) by a) 1D nanostructuring, b) 2D nanostructuring, c) 3D nanostructuring. Partly reproduced from Ref. [91,122], with permission from The Royal Society of Chemistry and The American Chemical Society.[90–92]

 © 2013 Wiley-VCH Verlag GmbH & Co. KGaA, Weinheim

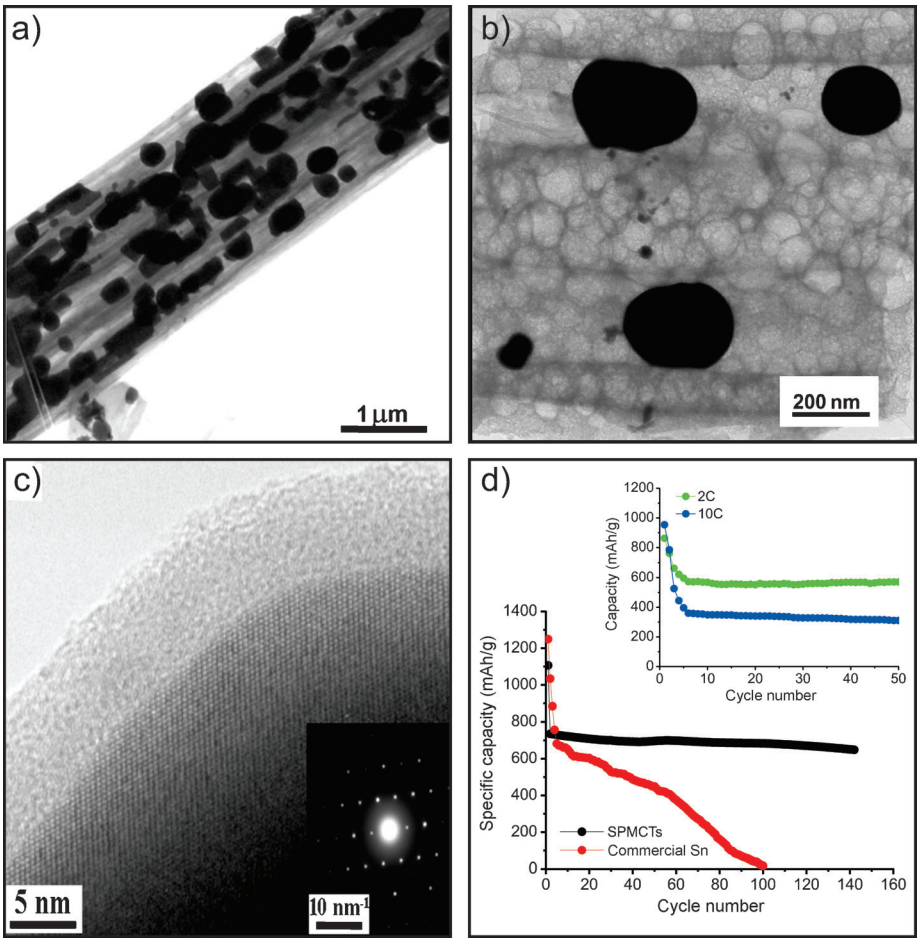

Figure 17. Tin nanoparticles embedded in carbon fibers (TEM). The mechanical decoupling of the individual particles combined with electrochemical coupling provides a greatly improved cycling performance compared to macroscopic bulk Sn. Reproduced from Ref. [91] with permission from The American Chemical Society.

carbon matrix to the Sn particles. 4) The Sn particles are mechanically decoupled (though electrochemically coupled, cf. (1), (2)), and volume variation is not a problem. 5) The carbon fiber acts as a binder holding the Sn particles together. 6) A transfer of Sn cations from the particles to the carbon and transport of them in the carbon is unlikely and thus so is electrochemical Ostwald ripening that would lead to grain growth. 7) It is probable that the carbon–electrolyte contact provides the necessary kinetic stability of the low-voltage situation.

As far as conversion storage and interfacial storage are concerned, kinetics plays a decisive role. In conversion storage the kinetics are extremely demanding and perhaps prevent this mechanism from being commercially used. In the interfacial storage, the situation is just the opposite. Here the favorable kinetics are an asset. This is impressively seen in Ref. [88], where the storage performance of nanoporous TiO_2 improves with increasing rate as the interfacial storage outperforms the kinetically complex bulk storage.

But back to the equilibrium consideration. The fact that nanoparticles are used and that multiparticle storage kinetics have to be addressed is also relevant for the Li distribution in single particles. Owing to the cost of interface formation, phase separation will be avoided in small crystallites if the macroscopically metastable mixed phase is not very high in energy (see e.g. Ref. [74]). Irrespective of this interfacial contribution, a digital storage mode (small particles either full or free of Lithium) is also expected for an ensemble of crystals in the system $LiFePO_4/FePO_4$ owing to the non-monotonic $\mu_{Li}(x_{Li})$ function.[100] These findings are also in agreement with the domino-cascade mode (storage in $FePO_4$).[101] An additional complication is related with the finding of long-range order (staging effects) in $LiFePO_4$.[78] Many of these subtleties, but also the high reversibility at the $LiFePO_4/FePO_4$ phase transition, can be ascribed to the very low excess free energies of the non-equilibrium compositions ("almost single phase storage").[102]

8. Defect Chemistry and the Search for New Materials

Unlike electronics, battery technology is a comparatively mature technology with clear-cut limitations. Correspondingly, the slope in a "Moore's plot" of available energy density versus time is flat. As far as lithium-based batteries are concerned, particularly the availability of improved electrode materials and the progress in nanotechnology pushed the field enormously.

It is clear that in principle, the combination $Li||F_2$ promises the highest theoretical energy density. Coupling with acid–base reactions could even increase voltage but at the expense of energy density.

Yet one should not forget that the major driving force for secondary batteries is that they are safe and highly reversible devices. The Li–air concept[103,104] is kinetically difficult on the cathode side (cf. kinetics of oxygen reduction, for example, in fuel cells) and it is hard to imagine how it could pass the enormous hurdles with respect to reversibility and safety for electromobility. Moreover the necessary catalysts for bringing the kinetics to a reasonable level will diminish the envisaged energy densities substantially. As recently reported,[105] the use of Au electrodes enabled a remarkable performance. Na–air batteries seem to function reasonably without costly and heavy precious metals.[106] $Li||S$ may be less delicate but offers a lower voltage[107] and still non-trivial redox kinetics. The related $Na||S$ cell[108] was long in the foreground of battery research. Its very good figures of merit were due to the fact that higher temperatures (300 °C) and thus liquid electrodes have been used separated by a ceramic electrolyte. Even though more and more highly conducting solid electro-

© 2013 Wiley-VCH Verlag GmbH & Co. KGaA, Weinheim

lytes become available,[109] for high-performance rechargeable batteries at room-temperature it is not probable that the electrolyte will be fully solid owing to the requirements of a good contact to the solid nanostructures. A variety of well-established liquid electrolytes, in particular based on alkylene carbonates, are available.[83,84] At extreme Li activities the stabilities rely on thin and flexible passivation layers which are usually ionically conductive, but not conductive for electrons.[83,84] Promising recent electrolyte developments include soggy-sand electrolytes or lithium-conducting polyelectrolytes that combine high conductivities and high cation-transference numbers with favorable mechanical properties.[89,110,111]

In terms of safety issues, ionic liquids are particularly interesting,[112] but appropriate solutions have not yet been developed. In the context of thermodynamics, electrolytes are only important here as far as they set boundary conditions in terms of stability.

As far as the selection of electrode materials is concerned the standard chemical potential of the phase is a primary thermodynamic search parameter. It is the decisive parameter for the voltage in two- or multiphase storage mode where eventually the standard Gibbs reaction energy counts, but it also gives an orientation with respect to the position on the voltage scale (around which then solubility effects provide variations). The search for appropriate phases is a major task of structural inorganic (or organic) chemistry, but it has also become a major target of computational chemistry and combinatorial synthesis.[113,114] Yet, when the equilibrium capacity is considered and even more so when practical energy density and power density are addressed, defect chemistry is important. In particular for the single-phase mode it is defect chemistry that governs the capacity as well as the voltage variation around the stoichiometric point. Here the mass–action constants for the relevant defect chemical reactions are the major determinants.

Let us, hence, for the rest of the Section consider, from a defect-chemical viewpoint, the most promising, classic storage mechanisms, in particular single-phase storage in view of the necessary materials quest. In essence, we are going to exploit the information of the equilibrium $\mathcal{E}$ versus δ diagrams (see for example, Figure 6), that are based on the defect-chemical diagrams.

While various solutions are offered with respect to the anode[26] problem (Si, Sn, etc. with theoretical capacities exceeding 1000 mA h g^{-1}),[115,116] it is striking that much fewer options seem to be in sight for cathodes.[26] (Of these only a very few have capacities exceeding 200 mA h g^{-1}.) In order to get a deeper insight let us discuss this aspect in the framework of a defect chemical analysis.

Besides chemical and crystallographic specificities there is one general point to be stated, that follows from Li incorporation (variation of μ_{Li}) meaning incorporation of both Li^+ (variation of μ_{Li^+}) and e^- (variation of μ_{e^-}). In ionic materials the first contribution refers rather to a crystallographic question (available sites), and is not fundamentally different for cathode and anode. This however is expected to be different for the second part, the accommodation of electrons. Therefore, the difference of anode and cathode on variation of μ_{Li} is especially reflected in the different variations of the μ_{e^-} values.

It is in intuitively clear that phases which are thermodynamically close to metallic lithium (in terms of μ_{Li}), that is, anode materials, have (typically) less problems to take up electrons without varying the voltage too much; the thermodynamic reason is the "electronic proximity" to lithium. This statement has to be taken with a pinch of salt as "proximity" to Li and interactions between ions and electrons also lead away from the ionic bonding picture. More generally, though, we might state that the Li incorporation can be split into the geometrical accommodation part and a part that subsumes the bonding questions, whereby the bonding question is decisive for the differences between cathode and anode.

Unlike anodic phases, in cathodic phases only a little addition of electrons (of course, along with incorporation of Li^+) to the highly oxidized phases may drastically increase μ_{Li} (in the single-phase mode) and hence decrease the voltage.[117] This sensitive dependence (which is usually mitigated by transition-metal elements) does not only lead to an unwanted steep voltage variation, the same effect (sensitive variation of the Gibbs energy) severely narrows the homogeneity range as the formation of competing phases is favored. For an anode a substantial increase of μ_{e^-} and finally μ_{Li} is prevented by the fact that the chemical potential of elemental Li forms the asymptote. Beyond that, the immediate phase neighborhood to lithium might lead to the case that a significant portion of the (e.g. interstitially) incorporated Li does not dissociate resulting in uncharged (interstitial) defects. The resulting compound tends to be less ionic and more metallic.

In fact, the large non-stoichiometries observed for Sn or Si require interactions between Li^+ and e^- to be favorable. In the ionic model they can be taken account of by activity coefficients and/or to a certain degree by introducing associates as new species. We will ignore such effects for the purpose of simplicity in the following.

The energies for accommodating Li^+ and e^- are contained in the mass–action constants of the defect chemical reactions, which we again will consider from the viewpoint of our simple LiX model system (cf. Figure 4).

To begin with, we simplify further and concentrate on the N regime, where Li is solely occupying interstitial sites (in Figures 18–21: $\delta \geq 0$) according to

$$Li + V_i \rightleftharpoons Li_i^\bullet + e' \tag{71}$$

Here Equation (31) applies which demands

$$\delta = K_{Li}^{1/2} a^{1/2} = K_F^{1/4} K_B^{1/4} \exp\left[-\frac{\mathcal{E}-\mathcal{E}^*}{2}\right] \tag{72}$$

The slope $d\mathcal{E}/d\delta = -2/\delta$ is infinite for $\delta = 0$ and diminishes with increased Li incorporation as long as the defects are dilute (see Figure 18). It is worthy of note to point out that a predominant neutral incorporation of lithium (Li_i^x) would lead to $\delta \propto a$ and hence to half the slope, that is $d\mathcal{E}/d\delta = -\delta$.

In Section 3 we considered $\mathcal{E}-\mathcal{E}^*$, that is, we referred to the intrinsic point (concentration of order).

© 2013 Wiley-VCH Verlag GmbH & Co. KGaA, Weinheim

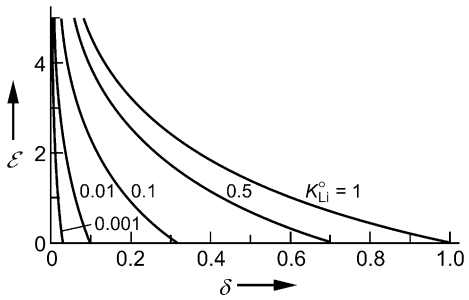

Figure 18. Voltage versus Li excess for different mass–action constants K°_{Li} (N-regime).

To judge the connection between the (normalized) voltage versus lithium $\mathcal{E}$ and the non-stoichiometry δ directly we make use of the fact that

$$a = e^{-\varepsilon}\frac{K^\circ_{Li}}{K_{Li}} \tag{73}$$

where K°_{Li} is the mass–action constant of the reaction in which we now start—in contrast to K_{Li}—from metallic Lithium Li(s):

$$Li(s) + V_i \rightleftharpoons Li_i^\bullet + e' \tag{74}$$

The term $\ln K^\circ_{Li}$ differs from $\ln K_{Li}$ by $-(\mu^\circ_{Li} - \mu^{\circ\circ}_{Li})/RT \equiv \ln K^{\circ\circ}_{Li}$ which is the negative standard Gibbs energy of bringing Li from the metal phase (reference electrode) to the working phase $(K^{\circ\circ}_{Li})$ (per RT). This value is positive and thus $K^{\circ\circ}_{Li} = K^\circ_{Li}/K_{Li} > 1$.

In spite of the fact that we refer to $\mathcal{E}$ directly (and not to $\mathcal{E}-\mathcal{E}^*$), we can directly use the Equations of Section 3 [Eqs. (33)–(49)], by replacing K_{Li} by K°_{Li}. Then the activity a transforms into an "absolute" activity given directly by $\exp(-\mathcal{E})$, whereby we have implicitly set $K^{\circ\circ}_{Li} = 1$ and identified μ°_{Li} with $\mu^{\circ\circ}_{Li}$.

If we, however, identify μ°_{Li} with μ^*_{Li}, that is the μ value at $\delta = 0$, then K°_{Li} includes the standard redox effect of bringing Li from the elemental phase to the ordered working phase (expressed by $K^{\circ\circ}_{Li}$), while K_{Li} only expresses the tendency to non-stoichiometry (specifically Li-excess).

Hence

$$\mathcal{E} = \ln\frac{K^\circ_{Li}}{\delta^2} = \ln\frac{K_{Li}K^{\circ\circ}_{Li}}{\delta^2} \tag{75}$$

Figure 18 shows that, given a certain practical $\mathcal{E}$ range, a high K°_{Li} value is favorable for extending the theoretical storage.

Equation (75) shows that δ is influenced by the voltage, and by K°_{Li} which can be decomposed into $K^{\circ\circ}$ and K_{Li}. As both $\mathcal{E}$ and $\ln K^{\circ\circ}_{Li}$ vary oppositely ($\ln K^{\circ\circ}_{Li}$ determines the standard potential) with the chemical distance from Li(s), they cancel each other out except for the configurational effects, leaving K_{Li} as major factor determining δ.

Realistically, the steep $\mathcal{E}$ increase for $\delta \to 0$ will be limited early on by:

a) purely internal effects, such as the change in the defect chemical regime, interactions, or site limitations
b) competition by other phases (such as Li-poor phases)
c) competition by other processes (such as oxidation of the electrolyte).

Let us concentrate on point (a) and emphasize that low Li non-stoichiometry favors domination by intrinsic disorder (ionic or electronic), that is, appearance of the I and E regimes. We will assume the appearance of the I regime by allowing for non-zero K_F (this also includes a finite value of μ°_V). Even though we consider the I regime we initially assume that we are still sufficiently far from the intrinsic point, so that we can concentrate on excess electrons ($\delta = i - v \simeq n$, that is, $K_B = 0$) as electronic carriers. We see from Figure 19 based on

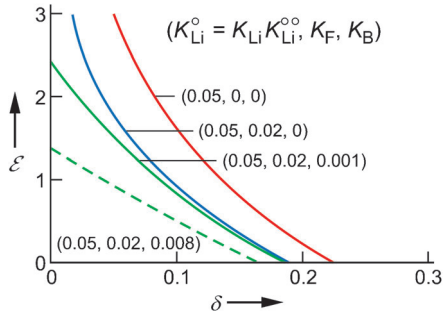

Figure 19. Voltage versus Li excess. N regime (red), N&I regime, but holes ignored (blue; cf. different K_F values), N&I regime including influence of holes (green) for two different band gaps (greater K_B corresponds to smaller band gap).

Equation (32) that the admixture of a non-zero K_F lowers $\mathcal{E}$ but also leads to a lower $\delta(\mathcal{E} = 0)$ value. This is because the Li^+-accommodation part of the stoichiometry change becomes thermodynamically more favorable. So the effect on storage capacity is ambivalent. If we also allow for a non-zero K_B, corresponding to finite formation energy of holes and then to a finite band gap, which also facilitates the electronic part of the stoichiometry change, we find a finite slope at $\delta = 0$. This deviation is quite significant at small δ referring to the fact that now another defect pair $(V'_{Li}, h^\bullet)$ can take over if δ changes sign.

The clear conclusion from these considerations is that low energies of excess (low μ°_i, μ°_n) or deficiency defects (low μ°_V, μ°_p) are important but high intrinsic ionic and electronic disorder (all relevant μ° values are low, that is, low K_F, K_B) is particularly favorable for flat electrode characteristics. (The favorable role of high disorder does not only refer to equilibrium, but is equally true as far as kinetics is concerned.)

Let us now address the whole defect chemical range (see Figure 22) and analyze the $\mathcal{E}$ versus δ curve as already given in Figure 6. The curve is based on the general expression given by Equation (33) for a pure material with the specification that it is intrinsically mainly ionically disordered (I regime) and at high deviations from the intrinsic point, the P and N regimes are established described by Equation (31). As far

© 2013 Wiley-VCH Verlag GmbH & Co. KGaA, Weinheim

as defect chemistry is concerned, Figure 4 and Figure 22 are relevant.

The curve is, on the δ-axis, confined by the values δ_{max} and δ_{min}, which are determined by the competition with other phases. The dashed line is calculated if site-exhaustion (or exhaustion of quantum states) is taken account of in the statistical treatment (ignoring interaction effects).

A closer look at Figure 6 reminds us that the absolute values of $\mathcal{E}$ depend on the Li incorporation energetics through K_{Li} which explicitly appears in $\ln a$; in addition the translation of $\ln a$ into the cell voltage involves the standard potential of Li in the phase under consideration (see labeling of y-axis of Figure 6). Unlike the values themselves the differences do not explicitly depend on Li incorporation energetics. The same is then true for the total available $\mathcal{E}$ range, whose extent is given by $\ln\left((\delta_{min}\delta_{max})^2/(K_F K_B)\right)$.

The information on Li storage defect thermodynamics (K_{Li}) however enters implicitly through the voltage values at the δ boundaries. At $\delta_{min,max}$ the Gibbs energy has changed, as a result of Li variation, to such an extent that it is favorable to form competing phases. As the Gibbs energy is the sum of the chemical potentials of all the regular and defective atomic contributions (see Appendices I, III), it is clear that the energy of lithium defects enters directly into the determination of δ_{min}, δ_{max} (but is of course not sufficient as contributions of competing phases are relevant as well).

It becomes again clear how important the intrinsic defect formation data are for the $\mathcal{E}$ range spanned by the phase. If the phase does not exhibit ionic ($K_F = 0$) or electronic disorder ($K_B = 0$) then the argument of the logarithm diverges meaning that the useful range around the stoichiometric point shrinks to zero (but compare Figure 19). On the other hand, large K_B, K_F values are not sufficient for a large $\mathcal{E}$ range owing to δ_{min}, δ_{max} being determined by the phase competition, and the information on how greatly the molar Gibbs energies of the other phases also vary with Li variation, is crucial (see also Appendix Ib). An interesting criterion for the steepness of the $\mathcal{E}$ decay on lithiation is the slope at the intrinsic point which is proportional to K_B^{-1} (ionic disorder) or K_F^{-1} (electronic disorder) [cf. Eq. (30)]. This means that a large ionic (electronic) disorder leads to a steep $\mathcal{E}$ variation if the tendency to electronically (ionically) disorder is small. The conclusion that favorable conditions for significant storage are high ionic disorder combined with a high electronic disorder has already been made.

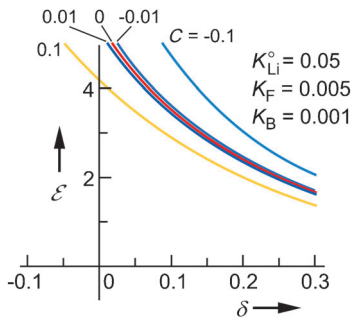

Figure 20. Effect of doping (acceptor: $C<0$, donor: $C>0$) on the $\mathcal{E}$ versus δ curve.

Figure 20 shows that for significant doping values (C values) the defect chemistry and hence $\delta(\mathcal{E})$ is similarly varied as it is the case for different mass–action constants. Special attention has to be paid to the fact that substantial inclusion of a foreign element alters the zero-point of the stoichiometry. Heavy doping by redox-active impurities (e.g. Fe^{3+}/Fe^{2+}) can increase Li solubility but only up to the dopant concentration (times the number of electrons involved in the redox step).[118]

We have already mentioned that even on heavy charging or discharging the number of available sites is usually not completely exhausted, instead, because the Gibbs energy of the phase will vary greatly, site occupation loses out in favor of transformation to a phase of lower Li content (extreme: X, for example, RuO_2) or higher Li content (extreme: Li). This is different if we consider the extreme phases X or Li itself, for which competing phases of lower or higher Li content, respectively, do not exist. The latter case is trivial, but the former case is interesting. Here no intrinsic Li disorder is possible, on charging a complete removal of Li (dissolved in X) is virtually possible (so Figure 18 fully applies). On discharge Li is dissolved, and—if the Li content is greater than $\sqrt{K_B}$—the N regime is established where $\delta = \sqrt{K_{Li}a}$. Of course on even extreme charging the reversible voltage will not be exceedingly high (formally $\mathcal{E}\to\infty$ for $\delta\to 0$). Here competing processes will usually limit the voltage, for example, electrolyte decomposition. But also other redox reactions may be perceived. Often if cells are freshly assembled with completely Li-free cathodes, for example, oxides, the initial voltage is typically determined by parasitic processes which are not sustainable. Such voltages break together as soon as a little lithium has been transferred.

If we can define a δ_{min} for the onset of a competing process, the N range experiences a two-sided limitation and according to Equation (31) gives

$$\mathcal{E}_{max} - \mathcal{E}_{min} = 2\ln(\delta_{min}/\delta_{max}) \tag{76}$$

again being independent of K_{Li}, as far as the explicit functionality is concerned, but being implicitly dependent on the Li incorporation energetics through the boundary values.

So far we concentrated on a single phase. Figure 21 shows how the voltage composition curve evolves if various phases

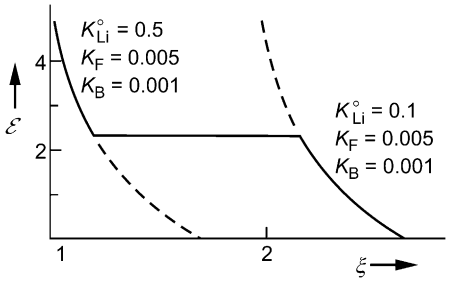

Figure 21. Generation of the two-phase situation (LiX–Li_2X). Since for simplicity we only considered N regimes, only Li excess situations are realized. The respective curves from Figure 19 have been shifted horizontally ($\delta\to\xi$) but also vertically as described in Appendix V. A more realistic curve is given by Figure 23.

© 2013 Wiley-VCH Verlag GmbH & Co. KGaA, Weinheim

are of interest. As an example, we select two $\mathcal{E}$–δ curves from Figure 18 the one with K°_{Li} =0.5 for the LiX and the one with K°_{Li} =0.1 for Li_2X. Transformation from δ to ξ by shifting the second curve to the right by 1 (relative to the first), renormalization of the concentration measure if necessary (Appendix V), and application of the two-phase equilibrium then leads to the bold lines. The reason why in Figure 21 the stoichiometric points are outside phase stability is due to the simplification that the initial curves only referred to N regimes. (Using the more realistic curves of Figure 22, one can easily reproduce realistic two-phase characteristics as sketched in Figure 23.)

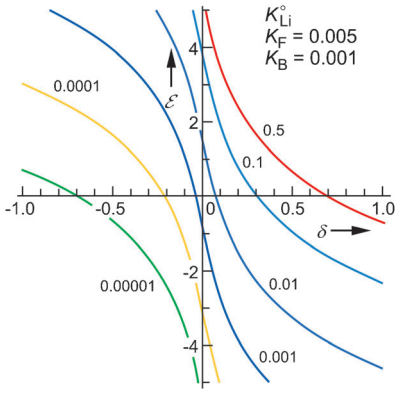

Figure 22. Voltage versus non-stoichiometry for pure LiX (N&I&P) showing the influence of the defect chemical parameters.

Figure 23 displays the breaking up of a virtual single-phase situation into a two-phase situation which leads to a smaller slope (ideally: horizontal in the two-phase range). Given the same $\mathcal{E}$ span, the great disorder that would be necessary in the single phase (small slope) is broken down into two phases of lower disorder (steeper slopes).

In this sense the two-phase mechanism which is characterized by a more constant $\mathcal{E}$ value, offers the advantage of being able to cover a large δ range which otherwise would require unrealistic mass–action constants. It is important to repeat here a statement from Section 5, namely that in the amorphous phase exactly this can happen.

The fundamental thermodynamical difference between bulk storage—where after all mass–action constants and hence combinations of μ° values are decisive for the thermodynamics—and interfacial space-charge storage (Section 6) is that in the space-charge case the individual μ° values matter. In other words: The restrictive condition of finding materials that store Li^+ and e^- in a desired voltage window is relieved by "job-sharing". Yet, naturally the specific capacity is reduced according to the fraction of interfaces.

As far as the search for appropriate junctions is concerned, one has, at the moment, to largely rely on semi-quantitative information and defect-chemical intuition, since individual chemical standard potentials are typically not known even for well-studied high-temperature materials.

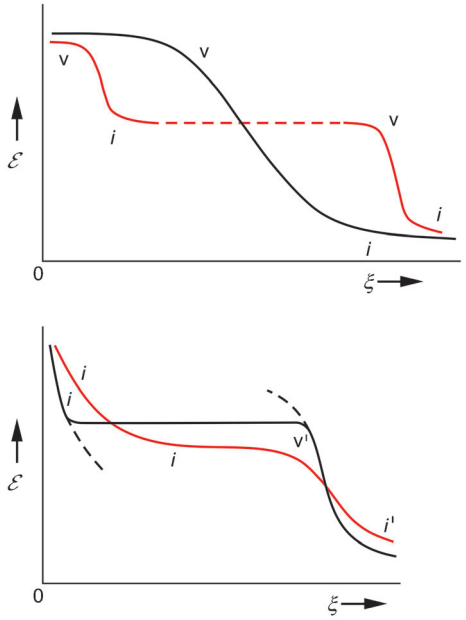

Figure 23. Two-phase storage allows a broad δ range to be covered for which in a single-phase mode unrealistic defect chemical parameters would be needed. Top: Comparison with a single phase whose concentration is between those of phases α and β and whose mass–action constants of disorder exhibit unrealistic values. Note that when generating these curves by varying K_F and K_B, the balance between K_{Li} and K'_{Li} needs to be considered.[40] Bottom: Coexistence of a boundary phase $Li_{\delta}X$ with a phase of higher Li content. Comparison with a phase in which high Li excess is possible and no miscibility gap occurs; here only interstitial defects occur. The first inflection point occurs through the exhaustibility of available sites [cf. Eq. (44)] rather than ordering. A further inflection point is possible by the occupation of a different class of interstitial sites (i'). This may be applicable to the amorphous state.

Combinations of standard chemical potentials (e.g. Frenkel enthalpy, Schottky enthalpy, band gap) are needed for a precise treatment of the classic storage modes, yet in the field of Li-battery materials this knowledge is—in spite of the significance—strikingly underdeveloped in comparison to high-temperature materials (e.g. for solid oxide fuel cells). It is to be hoped that the future development of the field will close this gap to favor a more thorough understanding of battery materials.

Herein the necessary thermodynamic aspects of electrochemical storage in solids have been set out. In addition the special aim of this article is to show that—also for battery research—a professional dealing with the solid state implies taking the mechanistic role of the point defects seriously. Additional insight becomes available not only for bulk problems but also for interfaces, not only for thermodynamically stable but also for metastable materials. In all the cases a thorough understanding is only achievable by addressing the charge carriers at the atomistic level. In turn, the solids' defect chemistry is able to guide us in the search for optimized electrodes.

© 2013 Wiley-VCH Verlag GmbH & Co. KGaA, Weinheim

Appendices I–V

Appendix I
The g–x and the Γ–ξ Representations

Before details are discussed it should be mentioned that in the case of surface contributions two definitions of the free enthalpy may be made. Either the total mechanical work (i.e. volume plus surface work) can be subtracted from the free energy or only the volume term is subtracted. Only in the first definition, to which we refer here, does it hold that $G=\Sigma\mu_i n_i$. For a thorough discussion see Ref. [57].

a) While (binary) mixture thermodynamics is usually formulated in terms of g versus x where g is the molar free enthalpy of mixing and x the mole fraction, in materials science it is often useful to refer to the Gibbs-energy per mole number of an invariant constituent (e.g. anion) and to the mole ratio[119] (e.g. cation to anion); we then write Γ and ξ. For a binary (A, B) it holds in the g versus x representation ($x_A=x$, $x_B=1-x$):

$$g=x\mu_A+(1-x)\mu_B,$$
$$\frac{dg}{dx}=\mu_A-\mu_B,$$
$$\mu_A=g+(1-x)\frac{dg}{dx}$$

These Equations are derived in all textbooks on chemical thermodynamics[120] and follow from $G=\Sigma_i n_i\mu_i$ and $\Sigma_i\mu_i dn_i=0$ implying $\Sigma_i n_i d\mu_i=0$ (p, T const.) in the equilibrium case.

If we now turn to Γ and ξ, the corresponding derivative is simply:

$$\frac{d\Gamma}{d\xi}=\mu_A$$

($\xi_A\equiv n_A/n_B\equiv\xi$). This follows from the definition of $\mu_A\equiv\left(\frac{\partial G}{\partial n_A}\right)_{n_B}$ as in $\frac{d(G/n_B)}{d(n_A/n_B)}$ the parameter n_B is a constant.

Since for $Li_\xi X$ it holds that $g=\Gamma(1-x)$ and $x=\frac{\xi}{1+\xi}$, that is, $1-x=\frac{1}{1+\xi}$, we also verify the necessary identity $g+(1-x)\frac{dg}{dx}=\frac{d\Gamma}{d\xi}$.

Hence in the g–x representation μ is obtained from the intercept of the tangent to $g(x)$ with the $x=1$ axis, whereas in the Γ–ξ representation μ is simply the slope.

Nonetheless in both representations, the double-tangent construction leads to the compositions of the two coexisting phases α, β. To demonstrate this we simply have to show that in both representations the slopes of the tangents at the two coexistence compositions are the same and equal to the slope of the line connecting these points.

In the g–x representation: The slope of this secant is given by $\frac{g^\beta-g^\alpha}{x^\beta-x^\alpha}$ which simplifies to $\mu_A-\mu_B$, since $\mu_A^\alpha=\mu_A^\beta$ and $\mu_B^\alpha=\mu_B^\beta$, clearly coinciding with the tangent slope.

In the Γ–ξ representation:

$$\frac{\Gamma^\beta-\Gamma^\alpha}{\xi_\beta-\xi_\alpha}=\frac{\xi_\beta\mu_A+\mu_B-\xi_\alpha\mu_A-\mu_B}{\xi_\beta-\xi_\alpha}=\mu_A=\mu_A^\alpha=\mu_A^\beta$$

Hence, again tangent and secant slopes are identical, and the double-tangent construction works here as well.

b) In the following the shape of the free-energy curves will be given for simple defect chemical regimes. For simplicity we concentrate on $\Gamma(\xi)$ and the compound $Li_{1+\delta}X$, that is, $\xi=1+\delta$. Extensivity of the G-function demands that

$$\Gamma=\mu_{LiX}+\delta\mu_{Li}\simeq\mu_{LiX}^\circ+\delta\mu_{Li}$$

which can be expressed in terms of defects. It is instructive to directly formulate this on the defect level.

The Gibbs energy for $Li_{1+\delta}X$ is given by

$$G=n_X\mu_{LiX}^\circ+n_i\mu_i+n_v\mu_v+n_p\mu_p+n_n\mu_n$$

plus contributions from association which we ignore here.

Simplifying because of $\mu_i=-\mu_v$ and $\mu_n=-\mu_p$ leads to

$$G=n_X\mu_{LiX}^\circ+(n_i-n_v)\mu_i+(n_n-n_p)\mu_n$$

Application of electroneutrality results in

$$G=n_X\mu_{LiX}^\circ+(n_i-n_v)(\mu_i+\mu_n)$$

As we ignore associates, it holds that $\delta n_X=n_i-n_v$, resulting in

$$G=n_X\left(\mu_{LiX}^\circ+\delta(\mu_i+\mu_n)\right)$$

or

$$\Gamma\equiv\frac{G}{n_X}=\mu_{LiX}^\circ+\delta(\mu_i+\mu_n)=\mu_{LiX}^\circ+\delta\mu_{Li}$$

Forming the derivative with respect to ξ or δ does lead back to μ_{Li} but up to a negligible term given by $2RT$ (since $\delta\mu_{Li}/d\delta\neq 0$; see e.g. the case discussed in Appendix III, there $\mu_{Li}=\text{const}+RT\ln\delta^2$ with $d\mu_{Li}/d\ln\delta=2RT$). This apparent inconsistency can be attributed to the neglect of the configurational entropy of the lattice molecule ($\mu_{LiX}-\mu_{LiX}^\circ$; cf. also Ref. [10]).

In the N regime: $\delta=n=i$, $\mu_{Li}=\mu_i+\mu_n$ and hence:

$$\Gamma=\mu_{LiX}^\circ+\delta\left(\mu_i^\circ+\mu_n^\circ\right)+RT\delta\ln\delta^2$$

The result in the P regime is analogous:

$$\Gamma=\mu_{LiX}^\circ-\delta\left(\mu_v^\circ+\mu_p^\circ\right)-RT\delta\ln\delta^2$$

In the I regime [cf. Eq. (30)]

$$\delta=2\sqrt{K_B}\sinh\left(\frac{\mu_{Li}-\mu_{Li}^*}{RT}\right)\equiv i-v=n-p$$

For $\mu_{Li}\simeq\mu_{Li}^*$, that is, $\delta\simeq 0$, δ can be approximated by

$$2\sqrt{K_B}\left(\mu_{Li}-\mu_{Li}^*\right)/RT=2\sqrt{K_B}\ln(a/a^*)$$

This yields a quadratic dependence

$$\Gamma=\alpha+\beta(\delta-\gamma)^2$$

with the minimum not being identical with $\delta=0$.

c) A parallel upwards shift of the molar Gibbs energy g to g' in Figure 12 gives rise to $\mu'_{Li}=\mu_{Li}+\Delta$. If the shift ($\Delta'$) in the Γ

© 2013 Wiley-VCH Verlag GmbH & Co. KGaA, Weinheim

versus ξ representation is a constant, $\mu_{Li} = \mu'_{Li}$ is the consequence (same slope). From the definitions of g, Γ, x, ξ it follows that $\Delta = \Delta'/(1+\xi)$. For $\Delta = \text{const.}$ it holds that $dg^{ex}/dx = 0$ while $d\Gamma^{ex}/d\xi = \Delta$ again showing that $\mu^{ex}_{Li} = \Delta$.
In the following this aspect is examined for the capillary effect in greater detail.
As shown in Appendix III it holds for $Li_\xi X = Li_{M+\delta}X$ (see also Appendix V)

$$g = \frac{\mu^\circ_{Li_M X}}{M+1+\delta} + \frac{\delta}{M+1+\delta}\mu_{Li}$$

$$g^{ex} = \frac{2\gamma}{r}\left[\frac{v_{Li_M X}}{M+1+\delta} + \frac{\delta}{M+1+\delta}v_{Li}\right]$$

(in the N regime with negligible $[Li^x_i]$ it is valid that $v_{Li} = v_i + v_n$; if $[Li^x_i] \gg i, n$ then $v_{Li} = v_{Li^x_i}$)

$$\Gamma = \mu^\circ_{Li_M X} + \delta\mu_{Li}$$

Introducing $x \equiv x_{Li} = n_{Li}/(n_{Li}+n_x)$, that is, $1 - x = \frac{1}{M+1+\delta}$ and $\xi = M + \delta$ leads to

$$g^{ex} = \frac{2\gamma}{r}\left[(1-x)v_{Li_M X} + (1-(M+1)(1-x))v_{Li}\right]$$

One recognizes that for "equipartition" of partial molar volumes $\left(v_{Li} = \frac{v_{Li_M X}}{M+1}\right)$ the x-dependence cancels. (If $M = 1$ then $v_{Li} = v_{LiX}/2$.) This is not the case in the $\Gamma(\xi)$ representation which then reads (see Appendix III)

$$\Gamma^{ex} = \frac{2\gamma}{r}\left[v_{Li_M X} + (\xi - M)v_{Li}\right] = \frac{2\gamma}{r}\frac{v_{Li_M X}}{1+M}(1+\xi)$$

Clearly in this approximation $g^{ex}(x) = \Delta = \text{const}$, while $\Gamma^{ex}(\xi) = \Delta(1+\xi) \neq \text{const}$. Forming the derivative $\frac{d\Gamma^{ex}}{d\xi}$ yields $\Delta = \mu^{ex}$ which is consistent with Equation (55). Hence the slopes in the $\Gamma^{ex}(\xi)$ representation are not identical but differ by a constant. Setting Δ' constant is the better approach if v_{Li} is negligible.
Generally neither Δ nor Δ' are constant (see Appendix III) and $\mu^{ex}_{Li} = \frac{2\gamma}{r}v_{Li}$. Moreover there will be also an implicit x-dependence, if the v values perceptibly depend on x.

Appendix II
Chemical Potentials of Phase, Component, and Defect

The chemical potential of the phase $Li_\xi X$ is

$$\mu_\alpha = \Sigma_j n_j \mu_j / n_\alpha = \Gamma_\alpha = g_\alpha(1+\xi)$$

where $n_j = $ mole number of component j, $\mu_j = $ chemical potential of component j in that phase.
For such a binary, the relation that connects g with x_{Li} has been given in Appendix I as

$$\mu_{Li} = g + (1 - x_{Li})\frac{dg}{dx_{Li}}$$

The relation between components and defects is given by[10,121]

$$\mu_{Li} = \mu\left(Li^x_i - V^x_i\right) = -\mu\left(V^x_{Li} - Li^x_{Li}\right)$$

Similarly

$$\mu_{Li^+} = \mu\left(Li^\bullet_i - V^x_i\right) = -\mu\left(V'_{Li} - Li^x_{Li}\right) \equiv \mu_i = -\mu_v$$

Appendix III
Partial Molar Volumes of Phase, Component, and Defect

At a first glance one might expect that $v_{Li} = \partial V/\partial n_{Li}$ is different from the volume effects generated by defect chemistry, this is however not the case. If the lithium is introduced as neutral interstitial it holds that $v_{Li} = v_{Li^x_i}$ as $dn_{Li} = dn_{Li^x_i}$. If the lithium is incorporated as $Li^\bullet_i + e'$ then $v_{Li} = v_i + v_n$ as $dn_{Li^\bullet_i + e'} = dn_{Li}$ (note that $\partial V/\partial n_{Li} \neq \partial V \Big/ \partial n_{Li^\bullet_i}$ as in the r.h.s. case, one charges the system). If , for example, $n\left(Li^\bullet_i + e'\right)$ pairs and subsequently $n(X'_i - e')$ pairs are introduced, then the $n\left(Li^\bullet_i + X'_i\right)$ pairs must reorganize in equilibrium to form normal lattice molecules since one refers to the initial stoichiometry again. As far as the volume effects are concerned, this ensures the extensivity of the total volume (linearity in v_{Li} and v_X).
Let us for the following consider just the N regime with negligible association, where all the Li excess is incorporated as i and n.
Then it correctly holds that

$$Li \rightleftharpoons Li^\bullet_i + e' \equiv \text{excess Li}$$

where the r.h.s. means the phenomenological lithium excess. For $i = n = \delta$ it holds that

$$\mu_{Li} = \mu_{Li(LiX)} = \mu^\circ_i(\infty) + \mu^\circ_n(\infty) + \frac{2\gamma}{r}(v_i + v_n) + RT\ln\delta^2$$

Clearly $v_{Li} = v_i + v_n$ and $a_{Li} \propto \delta^2$. (For neutral incorporation being dominant $a_{Li} \propto \delta$ would be the consequence.)
If we consider the constrained equilibria for different but fixed sizes, $\mu_{Li}(r) = \mu_i(r) + \mu_n(r)$ and $\mu_{Li}(\infty) = \mu_i(\infty) + \mu_n(\infty)$ then both situations do correspond to different equilibrium concentrations (e.g. $i(\infty) \neq i(r)$). But if we compare excess values at the same concentrations (same δ, that is, no equilibrium between both situations) then the concentrations are the same and cancel when forming excess values.
Let us refer to the N regime $\delta = i = n$, then according to Appendix Ic

$$\Gamma = \mu^\circ_{LiX} + \delta\left[\mu^\circ_i + \mu^\circ_n\right] + 2\delta RT\ln\delta$$

Writing this Equation for both r and ∞, realizing that $\mu^\circ(r) = \mu^\circ(\infty) + \frac{2\gamma}{r}v$ and forming the excess (the $\ln\delta$ term cancels), we obtain

© 2013 Wiley-VCH Verlag GmbH & Co. KGaA, Weinheim

$$\Gamma^{ex} = \left[\mu^{\circ ex}_{LiX} + \delta\left(\mu^{\circ ex}_i + \mu^{\circ ex}_n\right)\right] = \frac{2\gamma}{r}\left[v_{LiX} + \delta(v_i + v_n)\right] = \frac{2\gamma}{r}\left[v_{LiX} + (\xi - 1)(v_i + v_n)\right]$$

where $v_{Li} = v_i + v_n$. If this partial molar volume is positive (negative) the excess value increases (decreases) with δ. The excess chemical potential follows for constant v values as

$$d\Gamma^{ex} \Big/ d\xi = \frac{2\gamma}{r}(v_i + v_n) = \frac{2\gamma}{r} v_{Li}.$$

Similarly for g^{ex} one obtains

$$g^{ex} = \frac{2\gamma}{r}\left[\frac{v_{LiX}}{2+\delta} + \frac{\delta}{2+\delta} v_{Li}\right] = \frac{2\gamma}{r}\left[(1-x)v_{LiX} + (2x-1)v_{Li}\right],$$

and $\mu^{ex} = g^{ex} + (1-x)dg^{ex}/dx_{Li}$ again follows as $\frac{2\gamma}{r} v_{Li}$.
According to Appendix IV a rough approximation for the amorphous state assumes a capillary pressure effect, where r is replaced by r_0, that is, a radius of atomistic dimension (or by replacing the term with the free melting enthalpy under operational conditions). This applies to the free energy of the phase, and can act as a simple correction as far as the first term is concerned. Correcting the second term in the same way, would be grossly wrong.
Compared to a crystallized phase the amorphous phase will show excess tensile and compressive stress regions, which favor interstitial and vacancy defects formed at such distinguished positions.[73] An extreme value (minimum) would be the energy of defects in a melt (extreme, as in this case the relaxation is extreme). Since on the other hand the formation of electronic defects might be less favorable even the sign of the excess value is unclear. If the second contribution is expected to be distinctly negative this then would lead to a flat Γ curve in the amorphous case. In such a case, $\mathcal{E}$ would be increased compared to the crystalline case. Note that a flattening naturally is expected for large δ ($d\mathcal{E}/d\delta = -2/\delta$) and that this flattening is even more pronounced if Li_i^x associates occur. (If they are dominant: $d\mathcal{E}/d\delta = -1/\delta$.)
The approximation for Γ^{ex} then is

$$\Gamma^{ex} = \frac{2\gamma}{r_0} v_{LiX} + \delta\Delta\mu^{\circ}$$

where $\Delta\mu^{\circ} \equiv \Delta_R G^{\circ}$ is the reaction free enthalpy with R denoting $(i+n)_{crystalline} \rightleftharpoons (i+n)_{amorphous}$. The varied μ° values in the amorphous case can be translated into varied K values. Grossly increased ionic and electronic disorder would directly explain large non-stoichiometries (disappearing miscibility gaps) for amorphous situations. In this case the $\mathcal{E}(x)$ curve for an amorphous phase will not only be shifted but also smeared out compared with the curve for the crystalline phase.

Appendix IV
Energetic Rules of Thumb for Amorphous Materials

a) Melting point depression owing to capillarity ($w \equiv 2\gamma/r$; ℓ: molten, s: solid, m: melting point)

The Γ_l curve intersects the Γ_s and Γ_s' curves at T_m and T_m', respectively. It follows in linear approximation

$$\Delta T = T_m - T'_m = \frac{\Gamma_s(T_m) - \Gamma'_s(T'_m)}{-s_\ell}$$

$$= \frac{-T_m s_s + T'_m s_s - vw}{-s_\ell}$$

$$= (T_m - T'_m)\frac{s_s}{s_\ell} + \frac{vw}{s_\ell} = \Delta T \frac{s_s}{s_\ell} + \frac{vw}{s_\ell}$$

$$\boxed{\Delta T = \frac{vw}{s_\ell - s_s} = \frac{vw}{\Delta_m S}}$$

Note that Γ, s (entropy), h (enthalpy) refer to the total values of the phase LiX (G, S, H) divided by n_{LiX} (while g means the total value G divided by $n_{Li} + n_X$). As usual, reaction values (here values of the melting reaction, viz. $\Delta_m(G, H, S)$) refer to 1 mole of LiX as well.
b) Rule of thumb 1 (a: amorphous, ∞: infinite crystal)

$$\mu^{\circ a} - \mu^{\circ \infty} \simeq \Delta_m G = \Delta_m H - T\Delta_m S = (T_m - T)\Delta_m S$$

$$\boxed{\mu^{\circ ex} \simeq (T_m - T)\,\Delta_m S}$$

Here μ° is the standard potential of the phase $Li_{1+M}X$.
c) Rule of thumb 2 (r_0: radius of atomistic dimension)

$$\boxed{\mu^{\circ ex} \simeq v w_0}$$

$$w_0 \equiv w(r_0)$$

where γ is on the order of a grain boundary tension.
Here v is the molar volume of $Li_{1+M}X$.
d) If both rules are applicable, then

$$\boxed{T_m - T \simeq \frac{v w_0}{\Delta_m S}}$$

Comparison with the melting point depression formula shows that this is equivalent to stating that the crystallite size is so small that the melting point is virtually depressed to operational temperature (or roughly to 0 K, if $T \ll T_m$)

$$\boxed{T_m - T \simeq T_m - T'_m}$$

e) Relation for r_0 from the two rules of thumb

$$\boxed{r_0 \simeq \frac{v\,2\gamma}{(T_m - T)\,\Delta_m S}}$$

For $T \ll T_m$ r_0 is almost independent of T!
Order of magnitude consideration

© 2013 Wiley-VCH Verlag GmbH & Co. KGaA, Weinheim

$$r_0 \approx \frac{\upsilon 2\gamma}{T_m \Delta_m S} = \frac{\upsilon 2\gamma}{\Delta_m H}$$

For $\Delta_m H \simeq 20\ \mathrm{kJ\,mol^{-1}}$
$\upsilon \simeq 20\ \mathrm{cm^3\,mol^{-1}}$
$\gamma \simeq 0.2\ \mathrm{J\,m^{-2}}$
It follows that $r_0 \simeq 4$ Å. The examples considered so far suggest a value of r_0 in the range from 1 Å to 1 nm.
Note: The connection of μ°_{LiX} with μ_{Li} depends on the storage mode.
The connection of these results for $\mu^{\circ ex}_{LiX}$ with the excess e.m.f. of nanocrystals and hence $\mu^{ex}_{Li} = \frac{2\gamma}{r}\upsilon_{Li}$ requires multiplication by $\upsilon_{Li}/\upsilon_{LiX}$.
If we also use this scaling for amorphous materials, see the above rules of thumb, we obtain $\mu^{\circ ex}_{Li} = \Delta_m G \frac{\upsilon_{Li}}{\upsilon_{LiX}}$. As outlined in the text (see also Appendix III) this is not supposed to be a good approximation as the defect chemical situation between crystalline and amorphous materials is very different.
In the two-phase system μ^{ex}_{Li} is according to Equations (50) and (51) directly related with $\mu^{\circ ex}_{LiX} = \Delta_m G$. (The same result is arrived at if Equation (55) is applied and the term dg^{ex}/dx_{Li} replaced by the slope of the double tangent.)[70]

Appendix V
Concentration Measures

If in Li_2X we refer the non-stoichiometry to the number of regular Li in the Li sublattice we write $Li_{2+2\delta}X$ instead of $Li_{2+\delta}X$ (reference to the number of X sites). Both definitions of δ are different by a factor of 2 (number of regular Li/number of regular X). This difference expresses itself in a different configurational entropy which is finally reflected by a different concentration measure in the mass–action laws. If one uses the first definition, the selected curve for the N regime has, in addition to a horizontal shift by 1, to be shifted upwards by $2\ln 2$ (stemming from $\mathcal{E} = \ln K^{\circ}_{Li}/\delta^2$) as in Figure 21. This effect of the concentration measure can however be absorbed in the K values. This approach is generally advisable anyway as not just a vertical shift but a distortion of the curve occurs.

Acknowledgement

Discussions with Jörg Weißmüller and Marnix Wagemaker are acknowledged.

Received: July 13, 2012

[1] J. B. Goodenough in *Encyclopedia of Sustainability Science and Technology* (Ed.: R. A. Meyers), Springer, New York, **2012**, in publication.
[2] M. Armand, J. M. Tarascon, *Nature* **2008**, *451*, 652 – 657.
[3] P. G. Bruce, B. Scrosati, J. M. Tarascon, *Angew. Chem.* **2008**, *120*, 2972 – 2989; *Angew. Chem. Int. Ed.* **2008**, *47*, 2930 – 2946.
[4] J. Maier in *Die Zukunft der Energie*, *Die Antwort der Wissenschaft*, *Ein Report der Max-Planck-Gesellschaft* (Eds.: P. Gruss, F. Schüth), C. H. Beck, München, **2008**, pp. 282 – 294.
[5] J. Maier, *Nat. Mater.* **2005**, *4*, 805 – 815.
[6] J. Maier, *J. Power Sources* **2007**, *174*, 569 – 574.
[7] F. A. Kröger, *Chemistry of Imperfect Crystals*, North-Holland, Amsterdam, **1964**.
[8] F. A. Kröger, H. J. Vink, *Solid State Phys.*, *Vol. 3* (Eds.: F. Seitz, D. Turnbull), Academic Press, New York, **1956**, pp. 307 – 435.
[9] J. Maier, *Solid State Ionics* **2001**, *143*, 17 – 23.
[10] J. Maier, *Physical Chemistry of Ionic Materials*, *Ions and Electrons in Solids*, Wiley, Hoboken, **2004**.
[11] M. S. Whittingham, F. R. Gamble, *Mater. Res. Bull.* **1975**, *10*, 363 – 372.
[12] K. Mizushima, P. C. Jones, P. J. Wiseman, J. B. Goodenough, *Mater. Res. Bull.* **1980**, *15*, 783 – 789.
[13] A. K. Padhi, K. S. Nanjundaswamy, J. B. Goodenough, *J. Electrochem. Soc.* **1997**, *144*, 1188 – 1194.
[14] I. A. Courtney, J. R. Dahn, *J. Electrochem. Soc.* **1997**, *144*, 2045 – 2052.
[15] H. Li, X. J. Huang, L. Q. Chen, *Solid State Ionics* **1999**, *123*, 189 – 197.
[16] P. Poizot, S. Laruelle, S. Grugeon, L. Dupont, J. M. Tarascon, *Nature* **2000**, *407*, 496 – 499.
[17] P. Balaya, H. Li, L. Kienle, J. Maier, *Adv. Funct. Mater.* **2003**, *13*, 621 – 625.
[18] F. Badway, F. Cosandey, N. Pereira, G. G. Amatucci, *J. Electrochem. Soc.* **2003**, *150*, A1318 – A1327.
[19] H. Li, P. Balaya, J. Maier, *J. Electrochem. Soc.* **2004**, *151*, A1878 – A1885.
[20] J. Jamnik, J. Maier, *Phys. Chem. Chem. Phys.* **2003**, *5*, 5215 – 5220.
[21] Y. F. Zhukovskii, P. Balaya, E. A. Kotomin, J. Maier, *Phys. Rev. Lett.* **2006**, *96*, 058302.
[22] J. Maier, *Faraday Discuss.* **2007**, *134*, 51 – 56.
[23] N. A. Kaskhedikar, J. Maier, *Adv. Mater.* **2009**, *21*, 2664 – 2680.
[24] The fact that the energy input/gain is proportional to the difference in height h as the decisive parameter, even though the gravitational potential is proportional to $1/r$ (r being the distance between the centers of gravity of the masses) is not a contradiction. This is because h is defined relative to a zero-point R (sea level) such that $h \ll R$. Then the Taylor expansion gives $\frac{1}{R+h} \cong \mathrm{const} - h/R^2$.
[25] Storing the equivalent energy that is necessary to bring Li in a battery from the positive to the negative electrode at a voltage of 1 V, by motion of the same mass in the gravitational field, would require height differences that are not realizable on the earth surface.
[26] While the terms negative and positive electrodes are clearly defined as far as the material is concerned, the roles of anode and cathode change from charging to discharging. Herein we use the popular, but imprecise, convention to refer to the discharge and identify negative electrode with anode and positive electrode with cathode.
[27] Since they are chemically identical and of high electronic concentration, one can also consider the difference in the electrical potentials directly.
[28] This follows from the fact that in equilibrium there is no Li^+ flux ($j_{Li^+} \propto \sigma_{Li^+}\nabla\tilde{\mu}_{Li}$) implying a zero product of σ_{Li^+} (Li^+ conductivity) and $\nabla\tilde{\mu}_{Li^+}$ which for non-zero σ_{Li^+} means $\nabla\tilde{\mu}_{Li^+} = 0$.
[29] J. Maier in *Modern Aspects of Electrochemistry* (Eds.: B. E. Conway, C. G. Vayenas, R. E. White), Kluwer/Plenum, New York, **2005**, pp. 1 – 173; J. Maier in *Modern Aspects of Electrochemistry* (Eds.: B. E. Conway, C. G. Vayenas, R. E. White), Springer, New York, **2007**, pp. 1 – 138.

 © 2013 Wiley-VCH Verlag GmbH & Co. KGaA, Weinheim

[30] L. D. Burke, O. J. Murphy, *J. Electroanal. Chem. Interfacial Electrochem.* **1979**, *96*, 19 – 27.
[31] D. Muñoz-Rojas, M. Casas-Cabanas, E. Baudrin, *Solid State Ionics* **2009**, *180*, 308 – 313.
[32] See textbooks on chemical thermodynamics. If the chemical potential would decrease on increasing Li content, the equilibrium state would naturally not be stable with respect to variation of the Li amount.
[33] The chemical potential of lithium can also be expressed in terms of neutral Li defects ($\mu_{Li} = \text{const} + \mu_{Li_i^x} = \text{const}' + RT \ln[Li_i^x]$, dilute defects presupposed).
[34] We ignore substitutional incorporation as it 1) requires high mobility of the ion to be substituted and 2) would lead to complications on current reversal.
[35] C. Wagner, W. Schottky, *Z. Phys. Chem.* **1930**, *B11*, 163 – 210.
[36] C. Wagner, *Z. Phys. Chem.* **1936**, *B32*, 447 – 462.
[37] As far as the activity coefficients of point defect are concerned, the reader is referred to A. Lidiard, *Phys. Rev.* **1954**, *94*, 29 – 37.
[38] a) J. Maier, *Z. Phys. Chem.* **2005**, *219*, 35 – 46; b) J. Maier, *Z. Phys. Chem.* **2012**, *226*, 863 – 870.
[39] R. Merkle, J. Maier, *Phys. Chem. Chem. Phys.* **2003**, *5*, 2297 – 2303.
[40] For symmetry with Equation (21) it might be advisable to introduce a mass–action constant K'_{Li} defined by $[V'_{Li}][h^\bullet]a_{Li} = K'^{-1}_{Li}$. Note that $K_{Li}/K'_{Li} = K_F \cdot K_B$.
[41] R. Waser, *J. Am. Ceram. Soc.* **1991**, *74*, 1934 – 1940.
[42] J. Maier, *Phys. Chem. Chem. Phys.* **2003**, *5*, 2164 – 2173.
[43] P. Kofstad, *Nonstoichiometry, Diffusion and Electrical Conductivity in Binary Oxides*, Wiley, New York, **1972**.
[44] K. Hauffe, *Reaktionen in und an festen Stoffen*, Springer, Berlin, **1955**.
[45] G. Brouwer, *Philips Res. Rep.* **1954**, *9*, 366 – 376.
[46] N. Valverde, *Z. Phys. Chem.* **1970**, *70*, 113 – 127.
[47] R. Merkle, J. Maier, *Angew. Chem.* **2008**, *120*, 3936 – 3958; *Angew. Chem. Int. Ed.* **2008**, *47*, 3874 – 3894.
[48] S. R. Bishop, T. S. Stefanik, H. L. Tuller, *Phys. Chem. Chem. Phys.* **2011**, *13*, 10165 – 10173.
[49] J. Maier, R. Amin, *J. Electrochem. Soc.* **2008**, *155*, A339 – A344.
[50] J.-Y. Shin, D. Samuelis, J. Maier, *Solid State Ionics* **2012**, *225*, 590 – 593.
[51] J. Maier, *Phys. Chem. Chem. Phys.* **2009**, *11*, 3011 – 3022.
[52] P. Debye, E. Hückel, *Phys. Z.* **1923**, *24*, 185 – 206; P. Debye, E. Hückel, *Phys. Z.* **1923**, *24*, 305 – 325.
[53] For a *n*-component system $A_i^1 A_i^2 ... A_i^n$ for *i* running from 1 to 2, to be in complete equilibrium all the (*n*) chemical potentials $\mu(A^i)$ have to be the same. As one of these determines the cell voltage, the solution follows from the set of *n* equations with *n* unknowns. For an application of e.m.f. measurements in solid oxide electrolyte cells, see for example, W. Piekarczyk, W. Weppner, A. Rabenau, *Z. Naturforsch. A* **1979**, *34*, 430 – 436.
[54] N. A. Godshall, I. D. Raistrick, R. A. Huggins, *J. Electrochem. Soc.* **1984**, *131*, 543 – 549.
[55] For tiny sizes, the amorphous state can even be of lower Gibbs energy than the nanocrystalline state. This is the case whenever the surface free energy of the amorphous state is so much lower than the crystalline situation that the higher bulk free energy is overcompensated. See for example M. Pitcher, S. V. Ushakov, A. Navrotsky, *J. Am. Ceram. Soc.* **2005**, *88*, 160 – 167.
[56] R. Defay, I. Prigogine, A. Bellemans, H. Everett, *Surface Tension and Adsorption*, Wiley, New York, **1960**.
[57] A. I. Rusanov, *Phasengleichgewichte und Grenzflächenerscheinungen*, Akademie, Berlin, **1978**.
[58] J. Maier, *Adv. Mater.* **2009**, *21*, 2571 – 2585.
[59] J. Maier, *Solid State Ionics* **2002**, *154 – 155*, 291 – 301.
[60] T. L. Hill, *Thermodynamics of Small Systems*, W. A. Benjamin, New York, **1963**.
[61] D. Kramer, J. Weissmueller, *Surf. Sci.* **2007**, *601*, 3042 – 3051.
[62] Y. T. Cheng, M. W. Verbrugge, *J. Appl. Phys.* **2008**, *104*, 083521.
[63] L. D. Landau, E. M. Lifshitz, *Statistical Physics* (*Course of Theoretical Physics*), *Vol. 5*, Pergamon, Oxford, **1968**.
[64] Ref. [38a].
[65] P. Buffat, J.-P. Borel, *Phys. Rev. A* **1976**, *13*, 2287 – 2298.
[66] P. Knauth, G. Schwitzgebel, A. Tschöpe, S. Villain, *J. Solid State Chem.* **1998**, *140*, 295 – 299.
[67] A. Schroeder, J. Fleig, H. Drings, R. Wuerschum, J. Maier, W. Sitte, *Solid State Ionics* **2004**, *173*, 95 – 101.
[68] P. Balaya, J. Maier, *Phys. Chem. Chem. Phys.* **2010**, *12*, 215 – 219.
[69] C. Zhu, Ph.D. Thesis, Stuttgart, **2012**.
[70] O. Delmer, P. Balaya, L. Kienle, J. Maier, *Adv. Mater.* **2008**, *20*, 501 – 505.
[71] O. Delmer, J. Maier, *Phys. Chem. Chem. Phys.* **2009**, *11*, 6424 – 6429.
[72] While the interpretation of the e.m.f. in the two-phase reason in Ref. [70,71] is precise, the consideration of the single-phase regime based on a constant Δ overestimates the capillary effects, as outlined in this Section.
[73] D. Wagner, *J. Optoelectron. Adv. Mater.* **2004**, *6*, 345 – 347.
[74] M. Wagemaker, F. M. Mulder, A. Van der Ven, *Adv. Mater.* **2009**, *21*, 2703 – 2709.
[75] N. Meethong, H.-Y. S. Huang, S. A. Speakman, W. C. Carter, Y.-M. Chiang, *Adv. Funct. Mater.* **2007**, *17*, 1115 – 1123.
[76] J. Cahn, J. Hilliard, *J. Chem. Phys.* **1958**, *28*, 258 – 267.
[77] M. Wagemaker, B. L. Ellis, D. Luetzenkirchen-Hecht, F. M. Mulder, L. F. Nazar, *Chem. Mater.* **2008**, *20*, 6313 – 6315.
[78] L. Gu, C. Zhu, H. Li, Y. Yu, C. L. Li, S. Tsukimoto, J. Maier, Y. Ikuhara, *J. Am. Chem. Soc.* **2011**, *133*, 4661 – 4663.
[79] L. Suo, W. Han, X. Lu, L. Gu, Y. Hu, H. Li, D. Chen, L. Chen, S. Tsukimoto, Y. Ikuhara, *Phys. Chem. Chem. Phys.* **2012**, *14*, 5363 – 5367.
[80] Ref. [20].
[81] Ref. [5].
[82] J. Maier, *Prog. Solid State Chem.* **1995**, *23*, 171 – 263.
[83] E. Peled, *J. Electrochem. Soc.* **1979**, *126*, 2047 – 2051.
[84] D. Aurbach, *J. Power Sources* **2000**, *89*, 206 – 218.
[85] See for example, Ref. [82].
[86] J. Maier, *Ber. Bunsen-Ges. Phys. Chem.* **1985**, *89*, 355 – 362.
[87] S. R. de Groot, *Thermodynamics of Irreversible Processes*, North-Holland, Amsterdam, **1960**.
[88] J.-Y. Shin, D. Samuelis, J. Maier, *Adv. Funct. Mater.* **2011**, *21*, 3464 – 3472.
[89] A. J. Bhattacharyya, J. Maier, *Adv. Mater.* **2004**, *16*, 811 – 814.
[90] Y.-G. Guo, Y.-S. Hu, W. Sigle, J. Maier, *Adv. Mater.* **2007**, *19*, 2087 – 2091.
[91] F.-F. Cao, Y.-G. Guo, S.-F. Zheng, X.-L. Wu, L.-Y. Jiang, R.-R. Bi, L.-J. Wan, J. Maier, *Chem. Mater.* **2010**, *22*, 1908 – 1914.
[92] Y. Yu, L. Gu, C. Wang, A. Dhanabalan, P. A. van Aken, J. Maier, *Angew. Chem.* **2009**, *121*, 6607 – 6611; *Angew. Chem. Int. Ed.* **2009**, *48*, 6485 – 6489.
[93] Y. Yu, L. Gu, C. Zhu, P. A. van Aken, J. Maier, *J. Am. Chem. Soc.* **2009**, *131*, 15984 – 15985.
[94] H. Wu, G. Chan, J. W. Choi, I. Ryu, Y. Yao, M. T. McDowell, S. W. Lee, A. Jackson, Y. Yang, L. Hu, Y. Cui, *Nat. Nanotechnol.* **2012**, *7*, 309 – 314.
[95] Y.-S. Hu, P. Adelhelm, B. M. Smarsly, S. Hore, M. Antonietti, J. Maier, *Adv. Funct. Mater.* **2007**, *17*, 1873 – 1878.
[96] Y.-S. Hu, X. Liu, J.-O. Müller, R. Schlögl, J. Maier, D.-S. Su, *Angew. Chem.* **2009**, *121*, 216 – 220; *Angew. Chem. Int. Ed.* **2009**, *48*, 210 – 214.
[97] L. Bazin, S. Mitra, P. L. Taberna, P. Poizot, M. Gressier, M. J. Menu, A. Barnabe, P. Simon, J.-M. Tarascon, *J. Power Sources* **2009**, *188*, 578 – 582; M. Morcrette, P. Rozier, L. Dupont, E.

 © 2013 Wiley-VCH Verlag GmbH & Co. KGaA, Weinheim

Mugnier, L. Sannier, J. Galy, J.-M. Tarascon, *Nat. Mater.* **2003**, *2*, 755 – 761.
[98] A. R. Armstrong, G. Armstrong, J. Canales, R. Garcia, P. G. Bruce, *Adv. Mater.* **2005**, *17*, 862 – 865.
[99] S. Yang, X. Feng, L. Wang, K. Tang, J. Maier, K. Müllen, *Angew. Chem.* **2010**, *122*, 4905 – 4909; *Angew. Chem. Int. Ed.* **2010**, *49*, 4795 – 4799.
[100] W. Dreyer, J. Jamnik, C. Guhlke, R. Huth, J. Moškon, M. Gaberščček, *Nat. Mater.* **2010**, *9*, 448 – 453.
[101] C. Delmas, M. Maccario, L. Croguennec, F. Le Cras, F. Weill, *Nat. Mater.* **2008**, *7*, 665 – 671.
[102] R. Malik, F. Zhou, G. Ceder, *Nat. Mater.* **2011**, *10*, 587 – 590.
[103] P. G. Bruce, S. A. Freunberger, L. J. Hardwick, J. M. Tarascon, *Nat. Mater.* **2012**, *11*, 19 – 29.
[104] A. Débart, A. J. Paterson, J. Bao, P. G. Bruce, *Angew. Chem.* **2008**, *120*, 4597 – 4600; *Angew. Chem. Int. Ed.* **2008**, *47*, 4521 – 4524.
[105] Z.-Q. Peng, S. A. Freunberger, Y.-H. Chen, P. G. Bruce, *Science* **2012**, *337*, 563 – 566.
[106] P. Hartmann, C. L. Bender, M. Vračar, A. K. Dürr, A. Garsuch, J. Janek, P. Adelhelm, *Nat. Mater.* **2013**, 12, 228 – 232.
[107] X. Ji, K. T. Lee, L. F. Nazar, *Nat. Mater.* **2009**, *8*, 500 – 506.
[108] T. Oshima, M. Kajita, A. Okuno, *Int. J. Appl. Ceram. Technol.* **2004**, *1*, 269 – 276.
[109] N. Kamaya, K. Homma, Y. Yamakawa, M. Hirayama, R. Kanno, M. Yonemura, T. Kamiyama, Y. Kato, S. Hama, K. Kawamoto, A. Mitsui, *Nat. Mater.* **2011**, *10*, 682 – 686.
[110] A. Jarosik, C. Pfaffenhuber, A. Bunde, J. Maier, *Adv. Funct. Mater.* **2011**, *21*, 3961 – 3966.
[111] K.-D. Kreuer, A. Wohlfarth, C. C. de Araujo, A. Fuchs, J. Maier, *ChemPhysChem* **2011**, *12*, 2558 – 2560.
[112] M. Armand, F. Endres, D. R. MacFarlane, H. Ohno, B. Scrosati, *Nat. Mater.* **2009**, *8*, 621 – 629.
[113] G. Ceder, *MRS Bull.* **2010**, *35*, 693 – 701.
[114] G. H. Carey, J. R. Dahn, *ACS Comb. Sci.* **2011**, *13*, 186 – 189.
[115] A. Magasinski, P. Dixon, B. Hertzberg, A. Kvit, J. Ayala, G. Yushin, *Nat. Mater.* **2010**, *9*, 353 – 358.
[116] G. Derrien, J. Hassoun, S. Panero, B. Scrosati, *Adv. Mater.* **2007**, *19*, 2336 – 2340.
[117] The relationship mentioned at the end of Section 4 between the equilibrium oxygen partial pressure developed over non-variant systems and the cell voltage most impressively reflects the high degree of oxidation.
[118] Let us consider an n-type conductor for example. Concerning the variation of μ_{Li} with δ, the interesting term is $d\mu_{e^-}/d\delta$, the value of which is determined by χ_{con}/c_{con} where $c_{con} = [e']$ (J. Maier, *J. Am. Ceram. Soc.* **1993**, *76*, 1212 – 1217). χ_{con} is the electronic differential trapping factor of the valence change of the dopant which can be connected with the mass – action constant of the internal redox reaction and the doping content. If for the redox reaction $Fe^{3+} e^- \rightleftharpoons Fe^{2+}$, the free electron concentration can be considered as small compared to the concentration of the redox states, the term is proportional to $\frac{1}{[Fe^{3+}]} + \frac{1}{[Fe^{2+}]}$ which has a maximum for $[Fe^{3+}] = [Fe^{2+}] = m/2$. This expresses the buffer capacity as far as the electronic variation is concerned.
[119] There is considerable confusion in the literature concerning this issue.
[120] See, for example, C. H. P. Lupis, *Chemical Thermodynamics of Materials*, North-Holland, Amsterdam, **1983**.
[121] See, for example, W. Schottky, *Halbleiterprobleme I* (Ed.: W. Schottky), Vieweg, Braunschweig, **1954**.
[122] Y.-G. Guo, Y.-S. Hu, J. Maier, *Chem. Commun.* **2006**, 2783 – 2785.

© 2013 Wiley-VCH Verlag GmbH & Co. KGaA, Weinheim